REPUBLIC OF AZERBAIJAN

On the rights of the manuscript

ABSTRACT

Of the dissertation for the degree of Doctor of Sciences

COMPOSITION, STRUCTURE AND PROPERTIES OF NANOCOMPOSITES OBTAINED BY INTRODUCTION OF NANOPARTICLES INTO THERMOPLASTIC POLYMERS

Speciality: 2317.01- Nanochemistry and nanomaterials

Field of science: Chemistry

Applicant: **Flora Vidadi Hajiyeva**

Baku - 2022

The work was performed at the Department of "Chemical Physics of Nanomaterials" of Baku State University.

Scientific consultants: Academician,
                            Doctor of chemical science, professor
                            Abel Mammadali Maharramov
                            Doctor of physical science, professor

                            Mahammadali Ahmad Ramazanov

Official opponents: Correspondent members of ANAS,
                            Doctor of Chemical sciences, professor
                            Valeh Jabbar Jafarov
                            Correspondent members of ANAS,
                            Doctor of Chemical sciences, professor
                            Tofig Abbasali Aliyev
                            Doctor of Chemical sciences, professor
                            Eldar Isa Ahmedov
                            Doctor of Chemical sciences, professor
                            Nizami Allahverdi Zeynalov

Dissertation council under registration number BED 1.16/2 of the Supreme Attestation Commission under the President of the Republic of Azerbaijan, created on the basis of ED 1.16 of the Institute of Petrochemical Processes named after academician Y.G.Mamedaliyev of the National Academy of Sciences of Azerbaijan

Chairman of the Dissertation council:
                            Academician,
                            Doctor of Chemical sciences, professor
                            Vagif Majid Farzaliyev

Scientific secretary of the Dissertation council:
                            Doctor of Chemical sciences, Associate professor
                            Lala Mahammad Afandiyeva
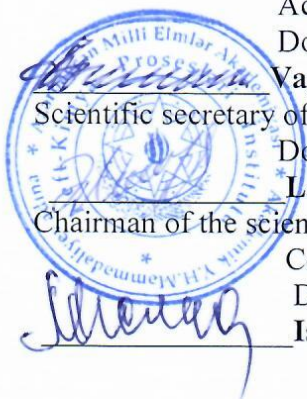
Chairman of the scientific seminar:
                            Correspondent members of ANAS,
                            Doctor of Chemical sciences, professor
                            Islam Israfil Mustafayev

GENERAL DESCRIPTION OF WORK

The relevance and degree of development of the topic. Currently, one of the promising areas in polymer science and materials science is the development and production of a fundamentally new class of materials - polymer nanocomposites. The unique properties of such nanocomposites are due not only to the extremely small sizes of nanosized particles but also to the structural features of the polymer matrix. The polymer matrix allows nanoparticles to be organized into supramolecular structures, which greatly enhances the unusual properties of nanosized particles. Polymer compositions with filler in the form of nanodispersed particles are promising for use as new conductive, photosensitive, magnetic, catalytic, and other materials that combine the properties of both a polymer medium and filler. Such materials exhibit optical, catalytic, magnetic, and sensory properties that are unusual in comparison with bulk materials. The advantage of such means is that it is possible to obtain both systems with low concentrations of nanoparticles in a polymer matrix, and systems with high concentrations of interacting particles. The properties of nanocomposites are determined by the chemical nature of the polymer matrix, the structure of interphase boundaries, the proportion of which in nanocomposites is huge, as well as the interaction between nanoparticles and the polymer matrix. These materials embody the properties of both a polymer matrix (flexibility, the ability to obtain elements of any configuration, etc.) and active filler (sensitivity). Individual components of nanocomposites can have magnetic, photoluminescent, photoresistive, electroluminescent and other properties, and compositions based on them exhibit completely new interesting properties[1].

The specific features of polymer nanocomposites are determined by both the individual properties of individual nanoparticles and the interaction of nanoparticles with each other and

---

[1] Pomogailo, A.D. Nanoparticles of metals in polymers / A.S. Rosenberg, I.E. Uflyand, - Moscow: Chemistry, - 2000.- 671 p.

with the matrix. We also note that by varying the properties of individual components, it is possible to vary the properties of nanocomposites, to study interphase boundary phenomena, the effect of interfacial interaction on the photoluminescent, magnetic, electret, and other active properties of the filler, and also to study the processes of intermolecular transfer and migration of electronic excitation energy in the polymer matrix.

Object and subject of research. The objects of research are thermoplastic polymers like isotactic polypropylene (PP), polyvinylidene fluoride (PVDF), magnetite nanoparticles Fe_3O_4, zirconium dioxide (ZrO_2), titanium dioxide (TiO_2), photosemiconductors of nanoparticles of cadmium sulfide (CdS), lead sulfide (PbS) and zinc sulfide (ZnS), metal nanoparticles of Cu, Fe, Co and Ni and multiwalle carbon nanotubes. The subject of the research is the development of new polymer nanocomposite materials based on the listed thermoplastic polymers and nanosized particles, the study of the structure and properties, the determination of the relationship between the structure and properties, as well as the prediction of possible areas of application of these materials.

Aims and objectives of the research: The aim of the research is to determine the optimal chemical technologies for the production and stabilization of metal nanoparticles, metal oxides, and sulfides, as well as to establish a relationship between the size of nanoparticles and the supramolecular structure of polymers, to study the mechanism of modification of electret, strength, magnetic and photoluminescent properties of polymer nanocomposites, as well as to study the possibilities the use of polymer compositions in various fields of technology.

The following tasks have been solved to achieve the goal:
1. Development of optimal chemical technologies for the production and stabilization of metal nanoparticles (Cu, Fe, Co and Ni);
2. Development of optimal chemical technologies for the production and stabilization of magnetic nanoparticles of mixed iron oxide - magnetite Fe_3O_4;
3. Synthesis and optimization of conditions for obtaining polymer

nanocomposites based on nanoparticles of metal oxides ZrO_2 and TiO_2;

4. Study of the influence of the technology of obtaining nanocomposites on the structure and properties of nanocomposites based on $PP+ZrO_2$ and $PVDF+ZrO_2$;

5. Investigation of the influence of the temperature-time regime of crystallization, heat treatment,and polarization processes on the morphology and photoluminescent properties of polymer nanocomposites based on $PP+ZrO_2$ and $PVDF+ZrO_2$;

6. Study of the influence of the method and conditions of polarization on the electret properties of nanocomposites based on $PP+TiO_2$ and $PVDF+TiO_2$;

7. Investigation of the influence of the technological method of obtaining polymer nanocomposites based on polypropylene and Fe_3O_4 nanoparticles on their structure, magnetic, electrophysical, and strength properties;

8. Study of the influence of the concentration and size of magnetic Fe_3O_4 nanoparticles on the structure and properties of magnetic polymer nanocomposites based on polyvinylidene fluoride and Fe_3O_4 nanoparticles;

9. Synthesis and stabilization of semiconductor nanoparticles of metal sulfides CdS, ZnS and PbS;

10. Influence of the supramolecular structure of polymers, temperature-time regime of crystallization, and heat treatment on the optical, photoluminescent, and dielectric properties of nanocomposites based on PP+PbS;

11. Influence of the technological factor on the structure and photoluminescent properties of hybrid nanocomposites based on PP+PbS/CdS;

12. Synthesis and study of optical properties of nanocomposites based on PVDF+CdS/ZnS;

13. Study of the possibilities of using polymer nanocomposites in various fields of technology.

Research methods: Complex physical and chemical experimental methods were used in the work: electrothermopolarization, polarization under the influence of corona

discharge, thermally stimulated depolarization, infrared spectroscopy, ultraviolet spectroscopy, scanning electron microscopy, transmission electron microscopy, atomic force microscopy, diffraction analysis, vibration magnetometry, photoluminescence, thermogravimetric method of analysis, differential scanning calorimetry, methods for measuring electrophysical and strength properties, compensation method for determining the density of electret charges, etc.

The main provisions for the defense:

1. It is shown that by varying the conditions of chemical deposition, including the nature and concentration of the surfactant, the concentration, ratio of the initial reagents, and etc. is possible to change the homogeneity, dispersion and purity of nanoparticles of metals of cobalt, nickel, iron, copper, iron oxide Fe_3O_4, sulfides of metals CdS, PbS and ZnS.

2. It has been shown that a change in the temperature-time regime of polymer crystallization, heat treatment, polarization conditions and other technological factors, as well as interfacial interactions between the components of the composites and the thickness of the interfacial layer, leads to a change in the photoluminescent, electrophysical, magnetic, electret and other active properties of nanocomposites.

3. It was found that in the polarization process of nanocomposites based on $PP+ZrO_2$, $PVDF+ZrO_2$, $PP+TiO_2$, and $PVDF+TiO_2$ under the influence of a corona discharge, the morphology of nanocomposites changes sharply, i.e. the size of the structural elements decreases. It was also shown that an increase in the luminescence intensity after polarization is due to the fact that, due to migration polarization, a large number of electric charges accumulate at the interface between the components of nanocomposites, and these charges create a high internal local field that excites in nanoparticles additional luminescent centers.

4. It was shown that for nanocomposites based on $PP+ZrO_2$ and $PVDF+ZrO_2$, in the region of destruction of crystalline phases of polymers due to an increase in the distance between nanoparticles, a sharp abrupt change in resistivity is observed, i.e. posistor effect is

observed.

5. It was found that, depending on the method and conditions of polarization, the value of the accumulated charge at the interface, the degree of interaction between the components of the nanocomposites and the thickness of the boundary layer change, which lead to a change in the electret and photoluminescent properties of nanocomposites based on $PP+TiO_2$ and $PVDF+TiO_2$.

6. It was shown that the structure-forming role of metal nanoparticles (Cu, Fe) and metal oxides (ZrO_2, Fe_3O_4) up to 3-5% content in polymer matrices is the reason for an increase in the thermal stability of nanocomposites based on these nanoparticles and polymer matrice PP.

7. It has been shown that a change in the mutual orientation of the magnetic moments of superparamagnetic Fe_3O_4 nanoparticles leads to the tunneling of charge carriers, which is the cause of the magnetoresistive effect in nanocomposites based on $PP+Fe_3O_4$ and $PVDF+Fe_3O_4$.

8. It has been found that an increase in the absorption capacity of magnetic nanocomposites at radio frequency wavelengths from 0.1 to 30 GHz is associated with an increase in the concentration of magnetic nanoparticles, the value of the intensity of the magnetic permeability and the tangent of the dielectric loss angle.

9. New hybrid photoluminescent polymer nanocomposites based on PP+CdS/ZnS and PVDF+CdS/ZnS have been developed and it has been shown that by varying the concentration of individual components of semiconductor clusters it is possible to vary the spectrally sensitive luminescence region.

10. New three-component, combined, electrically conductive,and magnetic radio-absorbing composite materials based on polyvinylidene fluoride with ferromagnetic nanoparticles of iron oxide Fe_3O_4 and multi-walled carbon nanotubes (MWCNTs) have been obtained and it has been established that high absorptions are observed in three-phase nanocomposites based on PVDF+ $5\%Fe_3O_4+10\%MWCNTs$.

The scientific novelty of the research:

1. The role of the introduction of nanosized metal fillers at low

contents into polymer matrices is revealed and their effect on the supramolecular structure, thermophysical, electrical, mechanical and magnetic properties of polymer nanocomposites is shown. It was found that at low concentrations of metal nanoparticles, metal oxides and sulfides in polymer matrices; they play the role of a structure former.

2. The effect of polarization under the influence of a corona discharge on the morphology and properties of nanocomposites based on $PP+ZrO_2$, $PVDF+ZrO_2$, $PP+TiO_2$ and $PVDF+TiO_2$ was established. The reasons for the increase in the photoluminescence intensity of nanocomposites are shown depending on the concentration and size of nanoparticles and the polarization conditions.

3. The role of accumulated charges in the boundary layer between the components of nanocomposites is revealed and it is shown that these charges, creating large internal local fields, contribute to the polarization of ZrO_2 nanoparticles, and this contributes to a large surface charge and charge life time.

4. The role of stabilized charges, the degree of interaction between the phases, the thickness of the boundary layer in the change in the electret and photoluminescent properties of nanocomposites based on $PP+TiO_2$ and $PVDF+TiO_2$ depending on the method and conditions of polarization, has been revealed.

5. The reasons for the increase in thermal stability of nanocomposites based on polypropylene filled with up to 3-5% content of metal nanoparticles and metal oxides (Cu, Fe, ZrO_2 and Fe_3O_4) have been identified. It has been established that up to 3-5% of the content of these metal nanoparticles and metal oxides in polymer matrices, nanoparticles play the role of a structure former.

6. It was revealed that nanocomposites obtained by hot pressing, in comparison with the extrusion method, are determined by the homogeneous distribution of the filler in the polymer matrix and the defect-free structure due to the influence of the technological factor on the formation of the supramolecular structure of nanocomposites.

7. It was revealed that the reason for the shift of the maximum crystallization temperatures of polymers towards high temperatures with an increase in the concentration of Cu, Fe and ZrO_2 nanoparticles in PP and PVDF polymer matrices is associated with the fact that nanoparticles play the role of nucleating agents, and this changes the supramolecular structure of polymers in nanocomposites.
8. It was revealed that the reason for the increase in the absorptive capacity of magnetic nanocomposites at radio frequency (0.1-30 GHz) wavelengths is associated with an increase in the concentration of magnetic nanoparticles, the intensity of magnetic permeability, the tangent of dielectric loss angle, which in turn lead to an increase in electromagnetic energy losses.
9. It was found that by varying the concentration of individual components of semiconductor clusters, one can vary the spectrally sensitive luminescence region of hybrid photoluminescent polymer nanocomposites based on PP+CdS/ZnS and PVDF+CdS/ZnS.
10. Combined, electrically conductive and radio-absorbing composite materials based on polyvinylidene fluoride with ferromagnetic nanoparticles of iron oxides and multi-walled carbon nanotubes (MWCNTs) were developed, and it was revealed that high absorptions are observed in three-phase nanocomposites based on $PVDF+5\%Fe_3O_4+10\%MWCNTs$.

The theoretical and practical significance of the research:

- The regularities of chemical production technologies established in the work make it possible to carry out a scientifically grounded choice of components to obtain new highly efficient composite materials with electrophysical, magnetic, magnetoresistive, electret, luminescent, photoresistive and operational properties for various purposes.
- Highly efficient nanocomposites based on polymers and nanoparticles of metals and metal oxides with high-performance properties have been developed.
- Elucidation of the influence of polymer crystallization conditions,

heat treatment, annealing of composition components, electrical treatment, and polarization processes on the structure, optical and photoluminescent properties of compositions is important for improving sensitivity, predicting and adapting properties, and determining the service life of composite converters.

- The created magnetic polymer nanocomposite films based on thermoplastic polymers and magnetite nanoparticles Fe_3O_4 were tested for the absorption of electromagnetic waves in radio frequency ranges.
- The possibilities of using polymer nanocomposites in various fields of technology have been studied.

Approbation and implementation:

Certain scientific provisions and results of the dissertation work were reported and discussed at the VII Republican Scientific Conference "Actual Problems of Physics", November 26, 2012, Baku, Azerbaijan; IV International scientific conference "Nanoscale systems: structure, properties, technology, Nansis-2013", November 19-22, 2013, Kiev, Ukraine; International Scientific Conference "Actual Problems of Physics" dedicated to the 80th anniversary of Academician B.M.Askerov, December 6, 2013, Baku, Azerbaijan; VIII International Conference "Nanostructures in Condensed Matter" October 7-10, 2014, Minsk, Belarus; Republican scientific conference "Actual problems of physics, December 17, 2015, Baku, Azerbaijan; I International Conference "Innovative Applications of Nanotechnology in Ecology, Nine-2016", March 20-23, 2016, Rome, Italy; Republican scientific conference "Actual problems of physics, December 22, 2016, Baku, Azerbaijan; I International Conference of Young Researchers dedicated to the 94th anniversary of National Leader Heydar Aliyev, May 05-06, 2017, Baku, Azerbaijan; International Scientific Conference "Modern Trends in Physics" April 20-22, 2017, Baku, Azerbaijan; International Scientific Conference "Problems of Physics and Astronomy", May 24-25, 2018, Baku, Azerbaijan; International Scientific Conference "Modern trends in Physics", May 01-03, 2019, Baku, Azerbaijan; VII International Scientific Conference "MTP-2021: Modern Trends in Physics", December 15-17, 2021, Baku, Azerbaijan.

Publications. The main results of the dissertation were published in 73 publications, of which 57 articles (including 43 papers in journals indexing in Web of Science Clarivate Analytics and 3 papers in Scopus database systems) and 16 are abstracts of the conference.

Name of the organization where the dissertation has been performed: The dissertation work, completed in the department of "Chemical Physics of Nanomaterials" of Baku State University.

Personal contribution of the author. The author outlines the main goals of the research and tasks for their achievement, defines the directions of research and carries out processing, systematization and discussion of the results. The author was also directly involved in the design and conduct of laboratory studies, in the development of probable mechanisms of the reactions carried out, as well as in the preparation of articles.

Volume, structure and the main content of the dissertation: The dissertation is presented on 380 pages of computer text (322868 characters) and consists of an introduction (19834 characters), six chapters (Chapter I- 64253 characters, Chapter II-57166 characters, Chapter III- 65929 characters, Chapter IV-44001 characters, Chapter V-41994 characters, Chapter VI- 24198 characters), main conclusions (5493 characters) and a bibliography of 251 items. The thesis is illustrated with 235 figures and 30 tables.

CONTENT OF WORK

The introduction substantiates the relevance of the work, formulates the goal and main tasks, and sets out the scientific novelty, the practical significance of the work, and the main provisions for the defense.

The first chapter is devoted mainly to the analysis of scientific literature; here the main methods of synthesis and stabilization of metal nanoparticles, metal oxides, and sulfides are considered, the influence of technological factors on the structure and properties of polymer nanocomposites is analyzed, as well as the

study of the active properties of polymer nanocomposites and the relationship between the structure and active properties of polymer nanocomposites.

From the analysis of the literature, the following conclusions were made:

• stabilization of nanosized metal particles by polymer macromolecules is due to the adhesive properties of the polymer to the metal, which depend on the physicochemical properties of the polymer and metal, the presence of functional groups and fillers, stabilizers in the polymer, the technology of obtaining metal-polymer composites and other factors. It was found that the adhesion of polymer molecules on the surface of nanosized particles saturates the reaction surface of the nanoparticles and creates a steric barrier for cluster growth.

• by varying the technological methods and conditions (pH-medium, temperature, nature of the solvent) for obtaining polymer nanocomposites, it is possible to obtain highly efficient materials with desired properties.

• active (photoluminescent, electret, magnetic), operational (electrical and mechanical strength, durability, aging under various external factors) and electrophysical properties of active polymer nanocomposites strongly depend on interfacial interactions between the components of the compositions, the nature of the polymer matrix (electronegativity, polarity, supramolecular structure), the properties of the filler, the processes of intermolecular transfer and migration of electronic excitation energy[2,3,4].

[2]Maharramov, A.M. Advanced Nanocomposites Types / A.M.Maharramov, M.A.Ramazanov, R.M.Saboktakin, - Nyu York: Nova Publisher,-2013. p.341.

[3]Ramazanov, M.A. Influence of Temperature and Time Crystallization Regime on the Strength Properties of Nanocomposites before and after Electrothermopolarization / M.A.Ramazanov, H.S.Ibrahimova // Integrated Ferroelectrics,- 2020. 212 (1), p.170-176

[4]Ramazanov, M.A. Influence of polarization processes on the charge states and dielectric properties of polyethylene-based compositions with low-molecular additions PE+PbCO$_4$ and PE+Cr/ M.A.Ramazanov, A.S.Quseynova // Optoelectronics and Advanced Materials-Rapid Communications,-2013. 7(9),-p.789-791.

The second chapter presents the results of the synthesis and stabilization of nanosized metal particles (Fe, Cu, Co, and Ni), new polymer nanocomposites based on nonpolar isotactic PP and polar PVDF thermoplastic polymers and nanosized particles of Fe, Co, Ni, and Cu metals are developed. The influence of the size of nanoparticles, the content of the nanofiller, and the type of polymer matrix on the morphology, strength, dielectric and thermophysical properties, as well as on the crystallinity of polymer nanocomposites based on metal nanoparticles has been investigated.

Figure 1 shows the diffraction pattern of iron nanoparticles synthesized by the method of chemical reduction of a salt of iron (III) chloride with sodium tetrahydroborate (NaBH$_4$) in the presence of a surfactant stabilizer, sodium oleate.
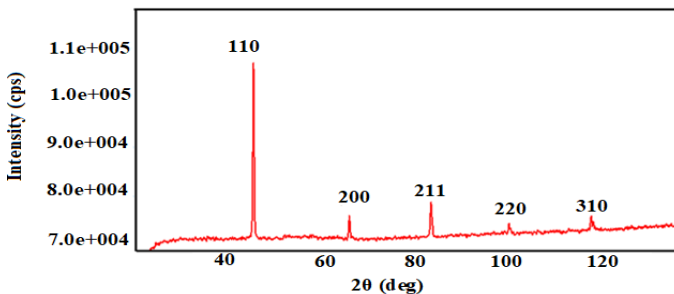
Fig.1. Diffraction pattern of iron nanoparticles.

Diffraction patterns were examined on a Rigaku Mini Flex 600 diffractometer using a copper anode X-ray tube (Cu-Kα radiation) at room temperature As can be seen from Fig.1., the main peaks at 2θ equal to 44.72^0 (110), 65.10^0 (200), 82.42^0 (211), and 116.43^0 (310) belong to iron nanoparticles, respectively, according of the database (ICDD no.00-006-0696). Figure 2 shows scanning electron microscopy (SEM) image (a) and energy dispersive spectrum (EDS) (b) of iron nanoparticles stabilizied in the presence of sodium oleate. SEM analysis was performed on a Jeol JSM-767 F scanning electron microscope. Energy dispersive micro-X-ray analysis was performed using the device X-Max 50 (Oxford Instruments). As can be seen from Fig.2., the average size of individual iron nanoparticles in the presence of sodium oleate is 10-13 nm. EDS spectrum also indicate

that the synthesized nanoparticles belong to iron nanoparticles. Iron nanoparticles were also obtained and stabilized in the presence of reverse micelles. It was found that the average size of iron particles synthesized in micellar solutions exceeds the diameter of nanoparticles synthesized in the presence of surfactants and is 19-44 nm, and the solution itself becomes cloudy with the formation of a precipitate.The main reason for this is the significant dynamic mobility of the micellar walls.
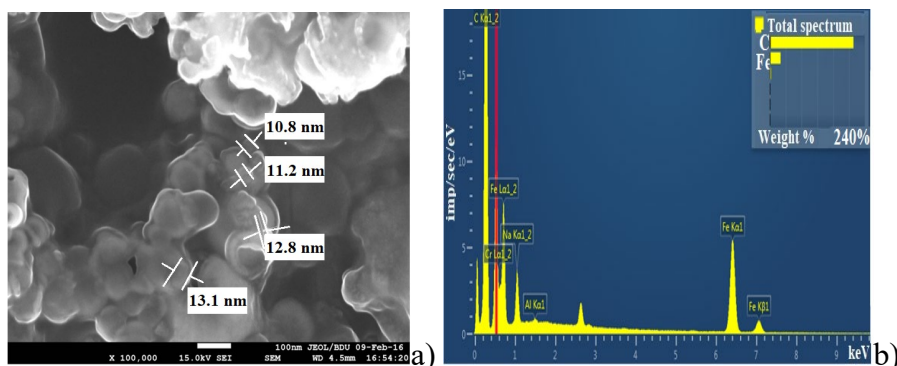

Fig.2. SEM image (a) and EDS spectrum (b) of iron nanoparticles stabilized in the presence of sodium oleate.

Figure 3 shows the diffraction pattern of copper nanoparticles synthesized by chemical reduction of copper sulfate with sodium tetrahydroborate in the presence of sodium oleate. The main peaks at 2θ equal to 42.94^0 (111), 50.71^0 (200) and 73.84^0 (220) belong to cubic copper nanoparticles. Furthermore, in the diffraction pattern at 2θ equal to 36.64^0 and 61.66^0 peaks, are observed belonging to particles of copper oxide CuO. It is assumed that the CuO particles are on the surface of the copper metal particles due to the partial oxidation of the copper. Based on the results of X-ray diffraction analysis, it can be concluded that the nanoparticles in the core consist of copper, and the surface layer is covered with a copper oxide shell. It was also found that the synthesized nanoparticles are well structured, and the amorphous phase is practically absent in the sample.
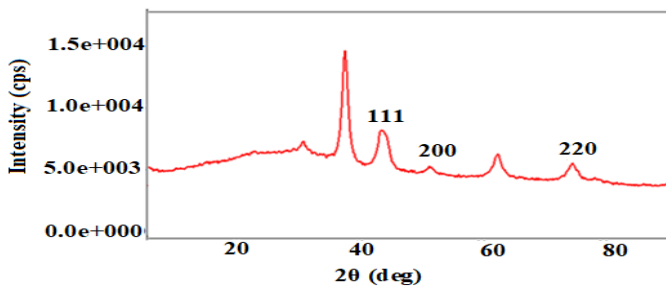
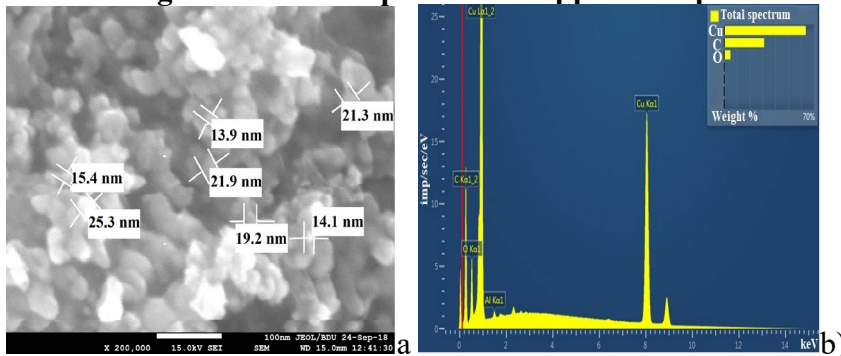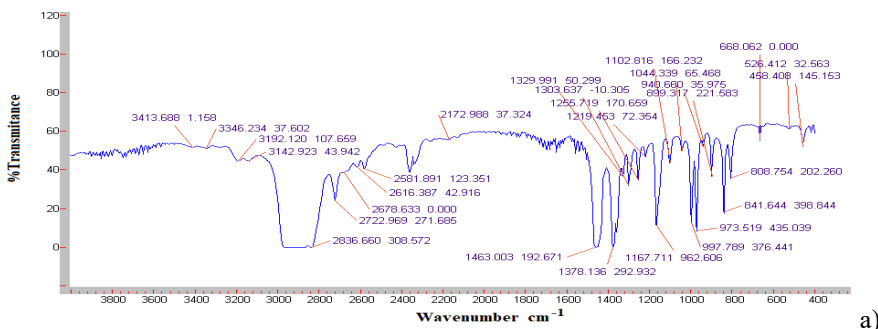**Fig. 3. Diffraction pattern of copper nanoparticles.**

Fig.4. SEM image (a) and EDS spectrum (b) of copper nanoparticles stabilized in the presence of sodium oleate.

Figure 4 shows the SEM image and EDS spectrum of copper nanoparticles synthesized and stabilized in the presence of sodium oleate. As seen from the SEM image, the average size of copper nanoparticles is 14-25 nm. EDS analysis also confirms that the synthesized and stabilized nanoparticles belong to copper nanoparticles.

a)

b)

c)

d)

Fig.5. IR spectra of pure PP (a) and nanocomposites based on PP+Ni (b), PP+Co (c), and PP+Cu (d).

Figure 5 shows the infrared (IR) spectra of pure polypropylene and nanocomposites based on PP and Cu, Co, Ni nanoparticles. IR spectra were recorded on a Varian 3600 FT-IR spectrometer in the range 4000-400 cm^{-1} at room temperature. It is known that absorption bands in the region of 2800-3000 cm^{-1} correspond to

16

stretching vibrations of CH_2 and CH_3 groups; absorption bands in the region of 1500-1300 cm^{-1} to deformation vibrations of CH_2 and CH_3 groups and absorption bands at 1200-800 cm^{-1} correspond to pendulum vibrations of CH_2 and CH_3 groups with stretching vibrations of the carbon skeleton of a polypropylene molecule. It was found that the introduction of Cu, Co, and Ni nanoparticles into the PP matrix decreases the intensities of many characteristic absorption bands of polypropylene in the range of 2800-3000 cm^{-1}, 1500-1300 cm^{-1}, and 1200-800 cm^{-1}. Consequently, the IR study of polymer nanocomposites based on PP and metal nanoparticles showed that the introduction of nanoparticles of the metals copper, cobalt, and nickel doesn't cause changes in the chemical structure of the polypropylene polymer, but only a change in the physical structure of the polymer occurs due to the interphase interactions of polypropylene with nanoparticles of nickel, cobalt and copper metals.

Figure 6 shows SEM images of nanocomposites based on PP+Cu depending on the content of Cu nanoparticles in PP. Have been established that with an increase in the content of Cu nanoparticles in the polypropylene matrix, agglomeration and aggregation of nanoparticles occurs. With the introduction of 1% Cu into the polymer, the average diameter of nanoparticles is 38-58 nm, and with 10% -is 40-73 nm.
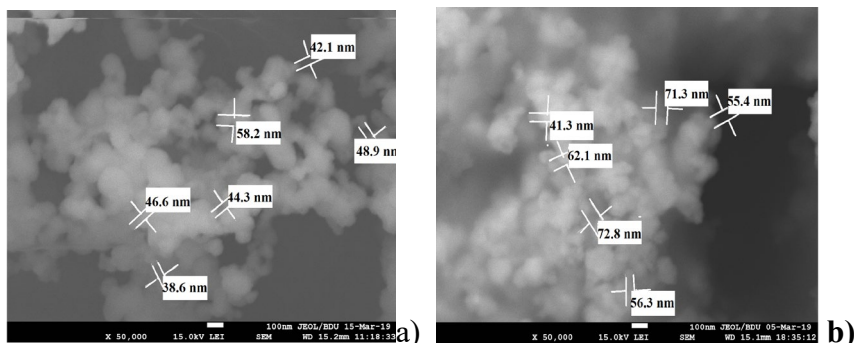

Fig. 6. SEM images of polymer nanocomposites based on PP+1%Cu (a) and PP+10%Cu (b).

Figure 7 shows atomic-force microscopy (AFM) 3D images of PP+Cu nanocomposites with different content of copper

nanoparticles. AFM images were taken using an Integra-Prima atomic force microscope (AFM) (NT-MDT, Zelenograd). A special silicon cantilever, prepared by plasma chemical method of etching with radius of curvature of needle 20 nm and resonance frequency 1–5 Hz was used. The measurements were performed in tapping microscopy mode in air, the changes in the oscillation amplitude of the cantilever needle that defines the surface topography was recorded. The scanning rate and scanning lines number on the image are 1.969 Hz and 256 Hz, respectively. Thus, at 1% Cu content in polypropylene, the distribution of Cu nanoparticles and the supramolecular structure are relatively more ordered than at high copper contents in the polymer. The AFM images also show that with a further increase in the copper content in the polymer, nanoparticles agglomerate in the matrix. This result correlates well with the average roughness of the polymer nanocomposite surface. Figure 8 shows the histograms of the root mean square roughness of the surface of nanocomposites based on PP+Cu. Thus, the average surface roughness for the PP+1%Cu nanocomposite is 20–80 nm; for PP+3%Cu-60-140 nm; for PP+5%Cu-50-150 nm. Hence, it should be concluded that, at low contents of Cu nanoparticles in the polymer matrix, the supramolecular structure of nanocomposites based on PP+Cu is more perfect than at high contents of nanoparticles in the polymer.
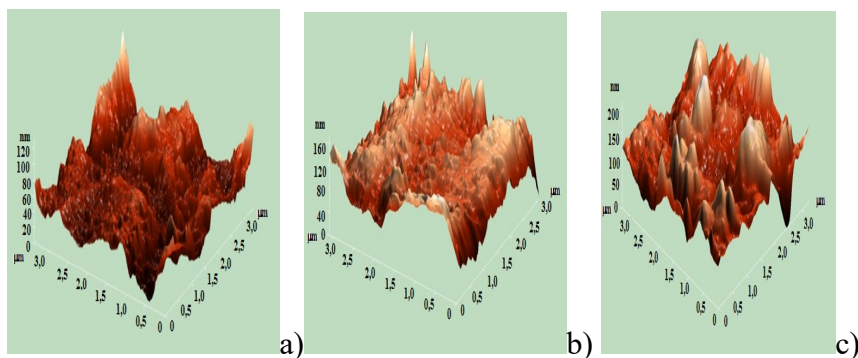

Fig. 7. AFM 3D images of polymer nanocomposites based on PP+Cu: a) PP+1%Cu, b) PP+3%Cu, c) PP+5%Cu.
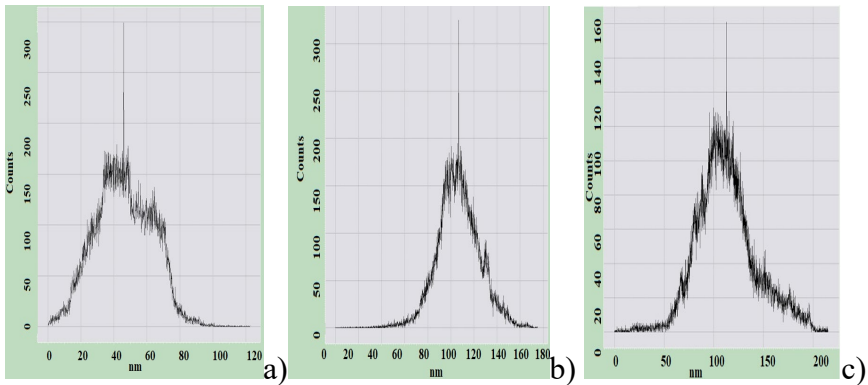
Fig. 8. Histogram of the image of the surface roughness of polymer nanocomposites based on PP+Cu: a) PP+1%Cu, b) PP+3%Cu, c) PP+5%Cu.

Figure 9 shows the thermogravimetric analysis (TGA) curves for pure polypropylene polymer and nanocomposites based on PP+Cu. Thermogravimetric (TGA) measurements of polymer nanocomposites were carried out in the temperature range $30-600^0$C for PP+Cu based polymer nanocomposites and $30-1000^0$C for PVDF+Cu based polymer nanocomposites at a heating rate of 20^0C per minute on a Seiko Exstar TG/DTA 6300 derivatograph (Japan). All curves show the initial thermo-oxidative destruction temperature at which the onset of weight loss is determined. It can be seen that PP begins to undergo thermo-oxidative degradation at a temperature of 257.06^0C with continuous weight loss up to 448.05^0 C. At a temperature of 448.05^0 C, 99% of the total polypropylene weight loss occurs. The area after 448.05^0 C corresponds to gradual weight. When Cu nanoparticles coated with a copper oxide layer is added to the polypropylene polymer matrix at 1% Cu content, the temperature of the onset of thermo-oxidative degradation for PP+Cu based nanocomposites shifts towards high temperatures and is 318.36^0 C. The mass loss continues continuously up to 479.13^0 C, after which the mass loss stops. With a 3% Cu content in PP, the temperature of the onset of thermo-oxidative degradation for polymer nanocomposites shifts to 330.33^0 C, and the weight loss continues up to 485.62^0 C.
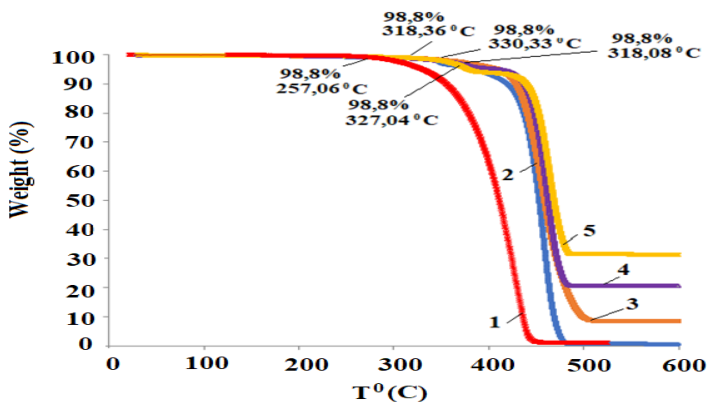
Fig.9. TGA curves of pure polypropylene (1) and nanocomposites based on PP+Cu: PP+1%Cu (2); PP+3%Cu (3); PP+5%Cu (4); PP+10%Cu (5).

A further increase in the Cu content in the polypropylene polymer matrix insignificantly decreases the temperature of the onset of thermo-oxidative degradation of polymer nanocomposites based on them. So, at 5% copper content initial thermo-oxidative destruction temperature for nanocomposites it is 318.08^0C and weight loss goes up to 480.55^0 C, and for 10% copper content - 327.04^0 C with continuous weight loss up to 481.56^0C. Consequently, it was found that the addition of copper nanoparticles to the PP polymer matrix increases the thermal stability of the polymer, and this thermal stability reaches its maximum value at a 3% content of copper nanoparticles in the polymer. A further increase in the content of Cu nanoparticles in the matrix leads to an insignificant decrease in $T_{destr.}$ towards low temperatures. TGA curves of polymer nanocomposites based on PVDF+Cu have been investigated (Fig. 10.). As can be seen from the TGA curves, for PVDF, the initial temperature of thermo- oxidative destruction begins at 428.57^0 C. With the introduction of Cu nanoparticles into the polymer matrix at a content of 3%, the initial thermo-oxidative destruction temperature is displaced towards low temperatures and is 378.89^0 C, with 5% copper content in the PVDF matrix initial thermo-oxidative destruction temperature is -372.67^0C. Consequently, the introduction of copper nanoparticles into the

PVDF matrix decreases the thermal stability of nanocomposites based on PVDF+Cu. The reason for the difference in the thermal properties of nanocomposites based on PP+ Cu and PVDF+Cu, in our opinion, is associated with the formation of a more perfect, dense and ordered structure of composites based on polypropylene than for PVDF.
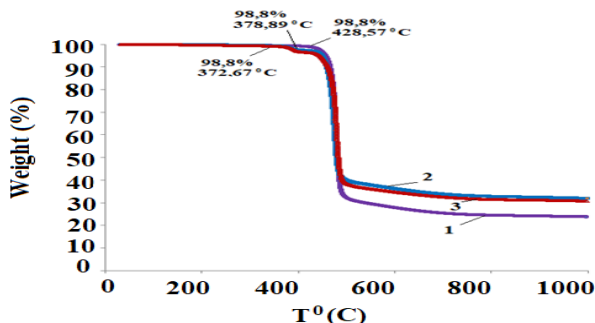

Fig.10. TGA curves of PVDF and nanocomposites based on PVDF+Cu: 1.PVDF; 2.PVDF+3%Cu; 3. PVDF+5%Cu.

All the results of thermogravimetric analysis of PP+Cu and PVDF+Cu based polymer nanocomposite samples are shown in Table 1. Table 1 also shows the values of the integral temperature at which destruction of almost 50% of the sample and the final temperature of thermo-oxidative destruction occurs.

Table 1.
Influence of copper nanoparticles on the thermal stability of polypropylene and polyvinylidene fluoride

Samples	$T_{onset.destr.}$ (^{0}C)	$T_{integ.}$ (°C)	$T_{fin.dest}$ (°C)
PP	257,06	410,95	448,05
PP+1%Cu	318,36	453,05	479,13
PP+3%Cu	330,33	458,75	485,62
PP+5%Cu	318,08	462,57	480,55
PP+10%Cu	327,04	468,84	481.56
PVDF	428,57	481,39	947,92
PVDF+3%Cu	378,89	478,69	979,45
PVDF+5%Cu	372,67	482,86	941,58

Figure 11 shows the differential scanning calorimetry (DSC) curves of melting (a) and crystallization (b) for nanocomposites

21

based on PP+Cu. DSC analysis was performed using a DSC 6100 differential scanning calorimeter (Seiko Instruments Japan). The heating and cooling rate were set at 10°C/min, and a high purity nitrogen with a flow rate of 70 mL/min was used to avoid oxidation of the samples, and 10 mg of each sample was first melted by heating up to 200°C from −40 °C (5 minutes hold), and then they were crystallized by cooling to −40 °C (5 minutes hold). It was found that with an increase in the content of Cu nanoparticles in the PP matrix, the melting point of nanocomposites decreases, while the crystallization temperature remains the crystallization temperature changes slightly. Figure 12 shows the DSC melting (a) and crystallization (b) curves for PVDF+Cu-based nanocomposites. It was found that with the introduction of copper nanoparticles into the PVDF matrix, the crystallization and melting temperatures of nanocomposites based on PVDF+Cu increase. It can also be seen that the crystallization temperature of polymer nanocomposites based on PVDF+Cu is significantly higher than of for the pure PVDF polymer. This shows that Cu nanoparticles are good nucleating agents in the PVDF matrix and leads to shift the peak of the crystallization temperature of nanocomposites based on PVDF+Cu towards high temperatures. It is known from the literature that only strong nucleating agents leads to shift the crystallization peaks towards high temperatures, while weak nucleating agents don't have this ability.
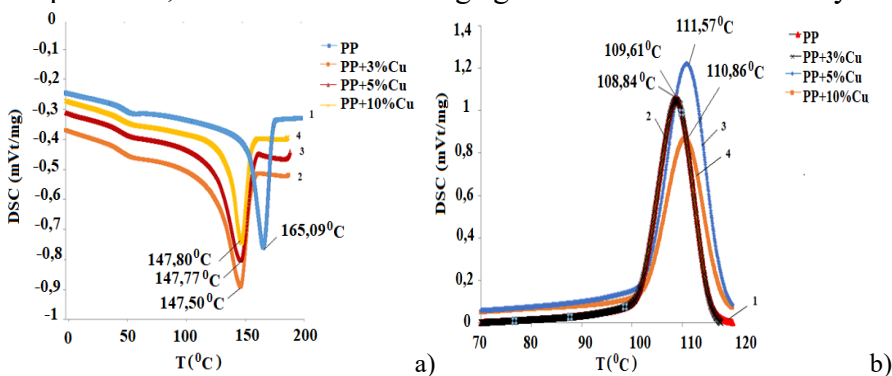

Fig.11. DSC curves of melting (a) and crystallization (b) for nanocomposites based on PP+Cu: 1. PP; 2. PP+3%Cu; 3. PP+5%Cu; 4.PP+10%Cu.
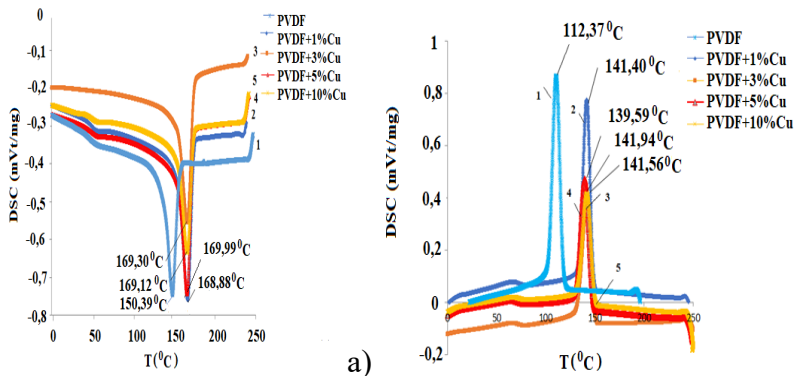
Fig.12. DSC curves of melting (a) and crystallization (b) for nanocomposites based on PVDF+Cu: 1. PVDF; 2. PVDF+1%Cu; 2.PVDF+3%Cu; 3. PVDF+5%Cu; 4. PVDF+10%Cu.

Also, from the DSC curves, from enthalpy of melting of nanocomposites the degree of crystallinity was calculated for polymer nanocomposites based on PP+Cu and PVDF+Cu (Table 2).

Table 2.

Results of DSC measurements obtained for nanocomposites based on PP+Cu and PVDF+Cu

Samples of nanocomposites	$T_{melt.}$ (^0C)	$T_{cryst.}$ (^0C)	Enthalpy of melting (C/g)	Crystallization degree (%)
PP	165,09	108,84	91,9	44.39
PP+3%Cu	147,50	109,61	76,56	36,98
PP+5%Cu	147,77	111,57	74,40	35,9
PP+10%Cu	147,80	110,86	60,93	29,43
PVDF	150,39	112,37	40,3	38,3
PVDF+1%Cu	168,88	141,40	56,62	53,9
PVDF+3%Cu	169,30	141,94	42,96	40,9
PVDF+5%Cu	169,99	139,59	45,04	42,8
PVDF+10%Cu	169,12	141,56	39,79	37,8

It was found that, with the introduction of copper nanoparticles into a polypropylene matrix, the degree of crystallinity of PP+Cu-based nanocomposites decreases for all concentrations of copper nanoparticles. For nanocomposites based on PVDF+Cu with the introduction of Cu nanoparticles into the PVDF matrix, the degree of crystallinity increases for all copper contents and reaches its

23

maximum value at 1% copper nanoparticles in the polymer. All the results of DSC measurements for nanocomposites based on PP+Cu and PVDF+Cu are given in Table 2.

Figure 13 shows the dependence of the specific magnetization of nanocomposites based on PP+Fe and PVDF+Fe on the magnetic field intensity. Magnetic measurements were performed using a vibration magnetometer (Quantum Design PPMS, Properties Measurement System, Quantum Design, Inc., USA). For nanocomposites based on PP+0.1%Fe and PVDF+1%Fe, the magnetic properties are negligible, which can be attributed to the low filler content and the diamagnetic contribution of the polymer.It was found that with an increase in the magnetic field intensity, the specific magnetization for polymer nanocomposites based on PP+10%Fe increases up to 90 emu/g, then saturation is observed.
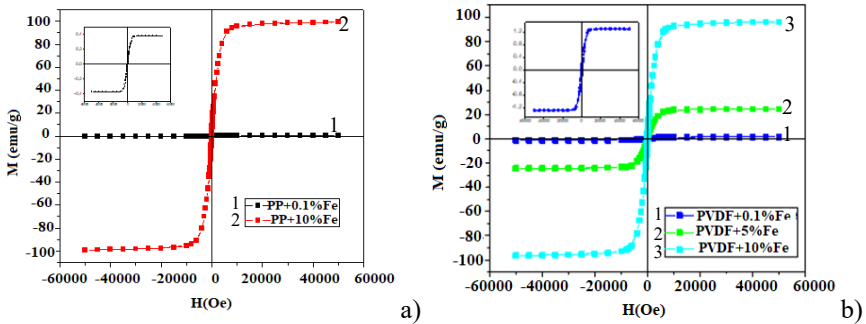

Fig. 13. Dependence of the value of specific magnetization for nanocomposites based on PP+Fe (a) and PVDF+Fe (b) at T = 300 K on the intensity of the magnetic field.

It was determined that with an increase in the magnetic field intensity, the specific magnetization for polymer nanocomposites based on PVDF+5%Fe increases to 20 emu/g, and for PVDF+10% Fe up to 90 emu/g, then saturation is observed. Thus, it has been shown that with an increase in the content of iron nanoparticles both in the PP matrix and in the PVDF matrix, the saturation magnetization increases. It was found that both for the nanocomposite based on PP+Fe and for PVDF+Fe near the zero point, residual magnetization is observed, i.e. hysteresis. Residual magnetization in these nanocomposites is explained by the fact that

24

iron nanoparticles have a non-single-domain structure in PP and PVDF matrices.

The third chapter presents the results of studies of the influence of technological factors of production and processing on the structure and properties of polymer nanocomposites based on thermoplastic polymers and nanoparticles of metal oxides. The effect of various types of polarization (electrothermopolarization, corona discharge, etc.), thermal annealing,and temperature-time regime of crystallization on the structure and photoluminescent properties of polymer nanocomposites has been investigated. The electret effect was discovered and studied in polymer nanocomposites based on PP, PVDF, and nanoparticles of zirconium dioxide (ZrO_2) and titanium dioxide (TiO_2). Figure 14 shows the dependences of the surface density of electret charges (σ) on the storage time (τ_{st}) of PP and PP+ZrO_2 polymer nanocomposites.
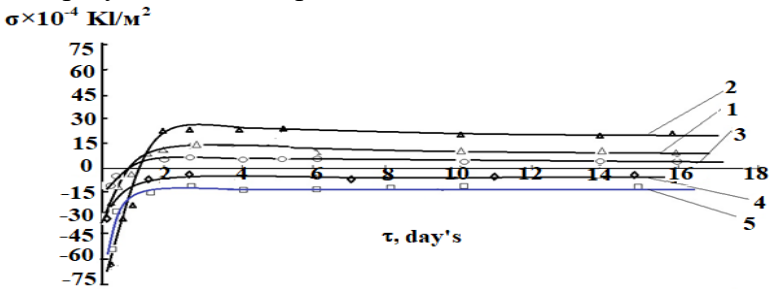

Fig.14. Dependence of the surface density of electret charges σ on the storage time τ_{st} of the composition:1. PP; 2.PP+1%ZrO₂; 3.PP+3%ZrO₂; 4.PP+5%ZrO₂; 5. PP+10%ZrO₂.

To measure the surface density of electret charges, polymer nanocompositions were first exposed to a negative corona. In the case under consideration, the polarization time of the samples was 300 s. After polarization, the total surface charge of the samples was immediately determined by the compensation method. In this case, the electrode, on the surface of which the electret is applied, is disconnected from the ground and an alternating voltage is applied to it. The polarity of the applied voltage is chosen opposite to the polarity of the electret charge. By adjusting the magnitude of the applied voltage, the magnitude of the signal induced from the electret

to the measuring electrode is brought to zero. Surface charge density is calculated by the formula (1):

$$\sigma = \frac{\varepsilon\varepsilon_0}{d} U_k \quad (1)$$

Where, ε- dielectric constant of polymer nanocomposite; ε_0- electrical constant; U_c- compensating voltage value; d- sample thickness.

It can be seen from the figure that after polarization of the polypropylene under the influence of a corona discharge, charges are accumulated in the sub-surface layer, and the polymer is charged with a homocharge. It can be seen that after 1.5 days these charges disappear, homocharges pass into hetero charges. It was found that for the PP+1%ZrO$_2$ ponanocomposite, the surface charge increases strongly, and the change in the homo- and hetero-charges is observed according to the same regularities. With an increase in the concentration of ZrO$_2$ nanoparticles in the polymer, there is a decrease in homo- and heterocharges; at a 5% content of ZrO$_2$ nanoparticles, heterocharges are not observed, but only homocharges are observed. For a nanocomposite based on PP+10%ZrO$_2$, the homocharge value and the charge lifetime are at their maximum. The method of thermally stimulated depolarization was used to predict the stability of electret charges, elucidate the reasons for the inversion of homo- and hetero-charges, and also to study the mechanism of their formation (Fig.15). Then, the thermally stimulated current (TSD) of the samples was recorded in the temperature range of 293-523 K under the condition of a linear increase in heating at a rate $\beta=4^0$C/min. From the TSD curves, the surface density of space charges, the values of the local electric field, the activation energy of charges and thickness of the interfacial layer for polymer nanocomposites based on PP+ZrO$_2$ were calculated (Table 3).

The intensity of the internal local field of injected charges for nanocomposites was calculated by the formula (2):

$$E_{loc.field} = \frac{\sigma}{\varepsilon\varepsilon_0} \quad (2)$$

where, $E_{loc.field}$- intensity of the internal local field of injected charges, σ- surface density of space charges, ε- dielectric constant of

nanofiller (ZrO_2), ε_0- electrical constant.

The interfacial layer thickness (δ) was calculated using the following formula (3):

$$\delta = \frac{2ne^2}{\varepsilon_1\varepsilon_2 kT}$$

(3)

where ε_1 и ε_2- dielectric constants of polymer and nanofiller, n-carrier concentration, e-electron charge, δ- interfacial layer thickness.

The activation energy of charges was calculated from the TSD curves by the method of the temperature position of the TSD current maxima. It was found that the activation energy for the $PP+ZrO_2$ based nanocomposites varies within 0.84-1.1 eV. The activation energy for the $PP+5\%ZrO_2$ nanocomposite is higher compared to other nanocomposites. It is shown that with an increase in the ZrO_2 concentration in PP, the thickness of the interfacial layer increases and reaches its maximum value at a 5% ZrO_2 content in polypropylene.
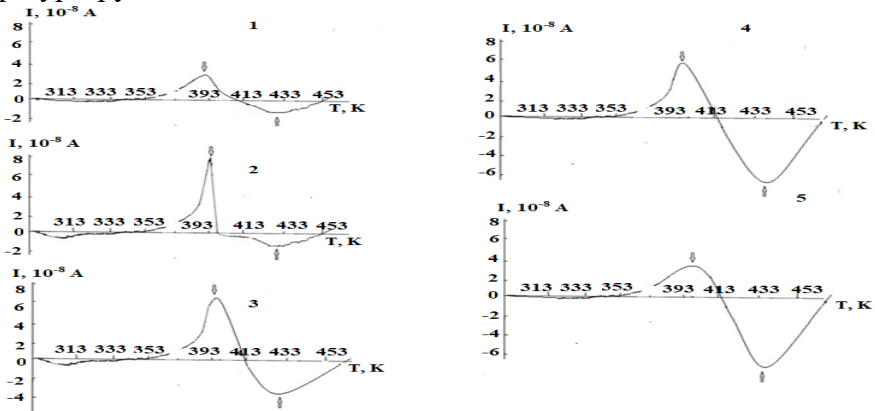

Fig.15. TSD curves of nanocomposites based on $PP+ZrO_2$ after polarization under the influence of a corona discharge at T=313K for 5 min: 1. $PP+1\%ZrO_2$; 2. $PP+3\%ZrO_2$; 3. $PP+5\%ZrO_2$; 4. $PP+7\%ZrO_2$; 5.$PP+10\%ZrO_2$.

As can be seen from Fig.15., the TSD curves exhibit two main maxima at temperatures of 393 K and 433 K, and the sign of these charges is opposite, i.e. polarization of the responsible homocharges and heterocharges occurs. It is known that

homocharges are responsible for the charges accumulated at the interface between the phases of nanocomposites, and hetero charges are responsible for dipole polarization. The number of homocharges was calculated from the TSD curves. It was found that the value of homocharges, depending on the concentration, changes with an extremum, i.e. the value of homocharges reaches its maximum value at 5% content of ZrO_2 nanoparticles in the polymer. It was experimentally established by the TSD method that, in the course of polarization, under the influence of a corona discharge, charges accumulate on the sample surface, these charges create a sufficiently large internal local field, and polarization of ZrO_2 nanoparticles occurs in the field of this charge.

Table 3.
Parameters calculated from TSD curves for nanocomposites based on PP+ZrO₂.

Nanocomposites	$\sigma \times 10^{-2}$ Kl/m²	$E_{loc.}$ (kV/m)	E_{activ} (eV)	δ (nm)
PP+1%ZrO₂	2,44	356	0,85	0,139
PP+3%ZrO₂	5,85	418	0,87	0,206
PP+5%ZrO₂	13,3	458	1,1	0,311
PP+7%ZrO₂	12,3	380	0,93	0,213
PP+10%ZrO₂	5,8	340	0,84	0,183

Have also been investigated TSD curves for polymer nanocomposites based on PVDF+ZrO₂. Have been determined that that for PVDF a maximum is observed at a temperature of 453 K; for the PVDF+5%ZrO₂ nanocomposite, two main maxima are observed at 447 K and 460 K. For the PVDF+10%ZrO₂ nanocomposite, three peaks are also observed at temperatures of 434 K, 447 K, and 460 K, and the sign of these charges for this nanocomposite is opposite, i.e. polarization of the responsible homocharges and heterocharges occurs. It was found that the value of homocharges, depending on the concentration, changes with an extremum, i.e. the homocharge value reaches its maximum value at 5% concentration of ZrO_2 nanoparticles in PVDF. Table 4 shows the values of the surface charge density accumulated at the interface between the components of the nanocomposites, the intensity of the internal field of the

injected charges, the activation energy of charges and thickness of the interfacial layer for PVDF+ZrO$_2$ based nanocomposites. Table 4 shows that in the process of polarization at the interface between the components of the PVDF+ZrO$_2$ nanocomposite, a large number of electric charges are accumulated. Thus, the intensity of the internal local field of injected charges for PVDF is 3.75 MV/m, for the PVDF+5%ZrO$_2$-39.89 MV/m and the PVDF+10%ZrO$_2$ nanocomposite - 37.36 MV/m. Were calculated the thickness of the interfacial layer for nanocomposites based on PVDF+ ZrO$_2$. It was shown that with an increase in the concentration of ZrO$_2$ in PVDF, the thickness of the interfacial layer increases and reaches its maximum value for nanocomposite based on PVDF+5%ZrO$_2$.

Table 4.
Parameters calculated from TSD curves for nanocomposites based on PVDF+ZrO$_2$.

Nanocomposites	$\sigma \times 10^{-4}$ Kl/m^2	E$_{loc.}$ (MV/m)	E$_{activ.}$ (eV)	δ (nm)
PVDF	8,29	3,75	1,26	-
PVDF+5%ZrO$_2$	88,25	39,89	1,25	12,49
PVDF+10%ZrO$_2$	72,75	37,36	1,55	11,67

The effect of a corona discharge on the structure and photoluminescent properties of polymer nanocomposites based on PP+ZrO$_2$ has been studied. The photoluminescence spectra were recorded on a Varian Cary Eclipse spectrofluorometer at a wavelength of 300-700 nm.
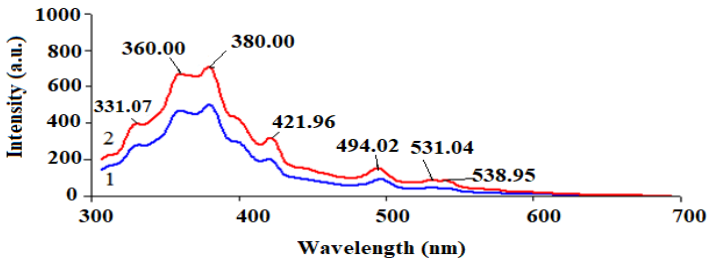

Fig. 16. Fotoluminescence spectra of the PP+1%ZrO$_2$ nanocomposite before (1) and after (2) polarization under the influence of a corona discharge.

Figure 16 shows the photoluminescence spectra of the

PP+ZrO$_2$ nanocomposite at concentrations of 1% before (1) and after (2) polarization under the influence of a corona discharge. It was found that after polarization the photoluminescence intensity increases, and the increase in the luminescence intensity depends on the concentration. It was found that under the influence of a corona discharge due to boundary charges, an internal local field of high intensity is created, and under the influence of this field, additional luminescent centers are excited in nan composites. The charges accumulated at the interface of the nanocomposite change the interfacial interactions, which lead to the excitation of luminescent centers in the nanoparticles, and this increases the luminescence intensity in the nanocomposites.

The surfaces of nanocomposites based on PP+ZrO$_2$ before (a) and after (b) polarization under the influence of a corona discharge at 5% content of ZrO$_2$ in a polypropylene matrix were studied by AFM microscopy. Figure 17 shows AFM 3D images of the PP+ZrO$_2$ nanocomposite before and after polarization under the influence of a corona discharge.
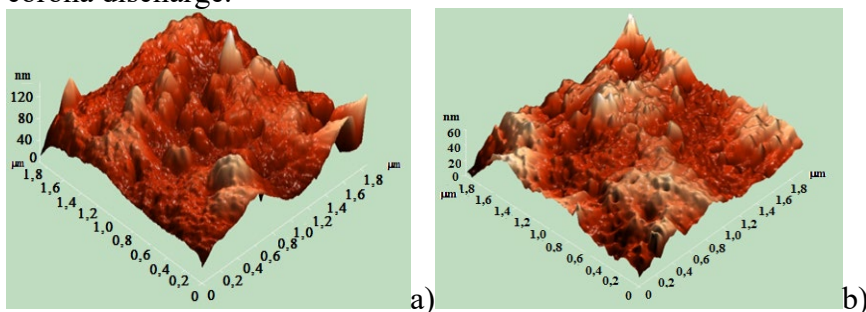

Fig. 17. AFM 3D images of the PP+5%ZrO$_2$ nanocomposite before (a) and after (b) corona polarization.

The AFM study of the relief of the samples of the PP+ZrO$_2$ composites shows that the relief of the samples of the composites changes greatly after polarization under the influence of a corona discharge. It can be seen that, after polarization of polymer nanocomposite samples, significant changes in their supramolecular structure occur. Figure 18 shows a histogram of image element values and rms surface roughness of PP+ZrO$_2$-based composites. As can be seen from the roughness histogram, after the polarization, the

relief of the compositions becomes relatively smooth. It was also shown that the root-mean-square roughness of the surface of the composites for unpolarized samples is 60-120 nm, and for polarized samples, it is 30-60 nm, i.e. after polarization, the structural elements are refined.
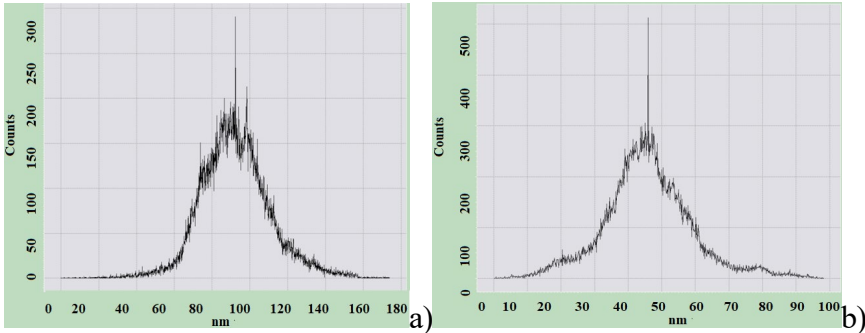

Fig.18. Histogram of the roughness of the PP+5%ZrO$_2$ nanocomposite before (a) and after (b) corona polarization.

The influence of other technological factors, including thermal annealing and temperature-time regime of crystallization, on the structure and photoluminescent properties of polymer nanocomposites based on PP+ZrO$_2$ and PVDF+ZrO$_2$ was also studied. It was found that, depending on the temperature-time regime of crystallization, a change in the photoluminescence intensity is observed. The change in the photoluminescence intensity at all wavelengths depending on the temperature-time regime of crystallization is explained by the activation of luminescent centers in ZrO$_2$ nanoparticles due to an increase in interfacial interactions between nanoparticles and the polymer. In the mode of slow cooling of polymer nanocomposites, larger molecular structures are formed, and this leads to a weakening of interactions with nanoparticles. In the rapid cooling mode, i.e., in liquid nitrogen, smaller crystallites are formed and nanoparticles play the nucleus of crystallization. As a result, stronger interphase interactions and, as a result, the photoluminescence intensity sharply increases. These results correlate well with the results obtained from AFM analyzes of polymer nanocomposites based on PP+ZrO$_2$ and PVDF+ZrO$_2$. Were also studied the photoluminescent properties of polymer

31

nanocomposites based on PP+ZrO$_2$ and PVDF+ZrO$_2$ after thermal annealing. It was found that the photoluminescence intensity for nanocomposites based on PP+ZrO$_2$ at all wavelengths increases with an increase in the annealing temperature to 120^{0}C, and for nanocomposites based on PVDF+ZrO$_2$ up to 140^{0}C. Possible reasons for a significant increase in the photoluminescence intensity after thermal annealing are the redistribution of charge carriers between levels in the band gap or the charge exchange of recombination centers and the removal of organic compounds adsorbed on the surface of nanocomposites.

The effect of polarization conditions on the charge state and electret properties of polymeric nanocomposites based on PP+TiO$_2$ has been studied. Figure 19 shows the dependences of the surface density of electret charges (σ) on the storage time (τ_{st}) for polymer nanocomposites based on PP+TiO$_2$ subjected to a corona discharge.
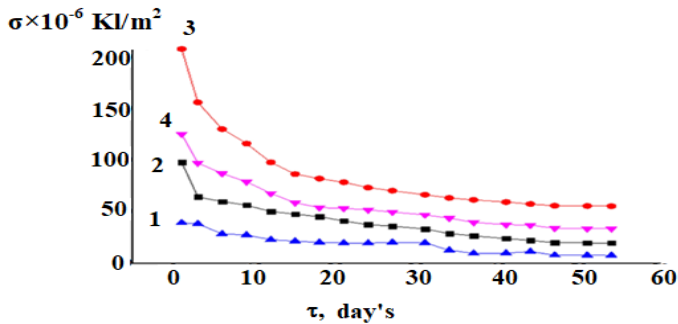

Fig.19. Dependence of the surface density of electret charges σ on the storage time τ_{st} of nanocomposites based on PP+TiO$_2$, subjected to corona discharge: 1. PP; 2. PP+0.5%TiO$_2$; 3.PP+1% TiO$_2$; 4. PP+3%TiO$_2$.

It can be seen from Fig.19 that with an increase in the TiO$_2$ content in polypropylene, the surface density of electret charges and the storage time measured by the induction method reach a maximum value at 1% of TiO$_2$ in polypropylene. The first studies of the dependence of surface density of electret charges σ on storage time showed that σ gradually decreases, and the character of the decrease in σ is different and depends on the TiO$_2$ concentration. Figure 20 shows changes in the surface density of electret charges σ

versus storage time τ_{st} of nanocomposites based on PP+TiO$_2$, subjected to the action of electrothermopolarization. It was found that the surface charge density for nanocomposites based on PP+1%TiO$_2$ subjected to electrothermopolarization is higher than for nanocomposites with a high filler content in the polymer matrix. It was also found that with an increase in the TiO$_2$ content in the matrix, the charge lifetime increases to 1% TiO$_2$ and then decreases.
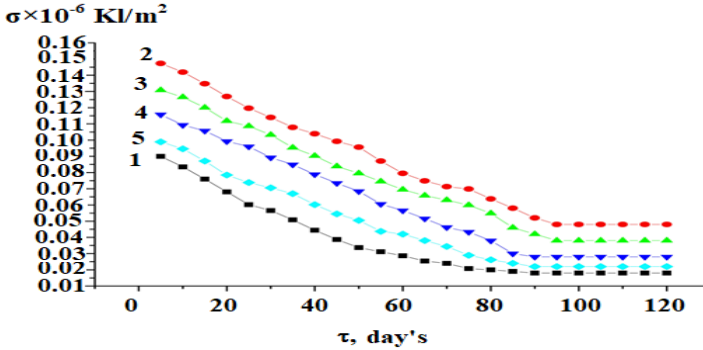

Fig.20. Dependence of the surface density of electret charges σ on the storage time τ_{st} of compositions subjected to electrothermopolarization at an electric field intensity Ep = 5×10⁶V/m: 1. PP; 2.PP +1%TiO₂; 3.PP+3%TiO₂; 4.PP+5%TiO₂; 5.PP+10%TiO₂.

It has been established that in the case of a corona discharge, the surface density of electret charges σ for nanocomposites based on PP+TiO$_2$ is higher than for nanocomposites subjected to the action of electrothermopolarization, and the stable electret charge for composites subjected to electrothermopolarization is higher than in the case of a corona discharge. In the case of polarization under the influence of electrothermopolarization, charges are accumulated at the interface both due to migration polarization and due to the injection of charge carriers with subsequent capture in polymer traps. In the case of a corona discharge, charges are accumulated only at the surface layer, creating a counter-field on the surface, which leads to quenching and relaxation of the corona charge. These results prove that the volume polarization charges play a significant role in the formation of the electret effect in composites, i.e., the change in the

33

electret properties of nanocomposite structures depending on the polarization regime is mainly associated with a change in the supramolecular structure of the polymer and the conditions for stabilization of charges in them.

The thermal properties of polymer nanocomposites based on $PP+ZrO_2$ and $PVDF+ZrO_2$ were also studied by TGA and DSC methods. It was found that the introduction of ZrO_2 nanoparticles at 1% content into the PP matrix shifts the temperature of oxidative destruction of PP towards high temperatures and is $296,86^0C$ (Table 5).

Table 5.
Influence of ZrO_2 nanoparticles on the thermal stability of polypropylene.

Samples	$T_{onset.dest.}$ (°C)	$T_{integ.}$ (°C)	$T_{fin.destr.}$ (°C)
PP	257,06	410,95	448,05
PP+1%ZrO_2	296,86	450	489,94
PP+3%ZrO_2	319,36	440	489,30
PP+5%ZrO_2	372,53	480	513,66
PP+10%ZrO_2	345,94	470	507,63

The loss of mass continues continuously up to a temperature of 489.94^0C, and then becomes a constant value. At a 3% content of ZrO_2 nanoparticles in PP, the temperature of the onset of thermooxidative degradation shifts to 319.36^0C and the weight loss continues continuously up to 489.30^0 C. At a 5% content of ZrO_2 nanoparticles, the temperature of the onset of thermooxidative degradation shifts to 372.53^0C and the weight loss continues continuously up to 513.66^0C. A further increase in the content of ZrO_2 nanoparticles shifts the temperature of the onset of thermooxidative degradation towards low temperatures. Thus, at a 10% content of ZrO_2 nanoparticles, the temperature of the onset of destruction is 345.94^0C and the weight loss continues up to 507.63^0C. Thus, the introduction of ZrO_2 nanoparticles into the PP matrix increases the thermal stability of the PP. Taking into account that PP is a one of widely used industrial thermoplastic polymers, therefore, it can be concluded that an increase in the thermal stability

of polypropylene by $115,47^0$C (for PP+5%ZrO_2 nanocomposite) will expand the possibilities of using polymeric nanocomposites based on PP+ZrO_2.

TGA analysis of nanocomposites based on PVDF+ZrO_2 showed that when ZrO_2 nanoparticles are introduced into the PVDF polymer matrix with their content of 3% in the matrix, the temperature of the onset of thermal oxidative destruction shifts towards low temperatures and is 296.2^0C; at a 5% ZrO_2 content, the temperature of the onset of thermal oxidative destruction is 263.3^0 C. It was found that the introduction of ZrO_2 nanoparticles into the PVDF matrix decreases the thermal stability of nanocomposites based on PVDF+ZrO_2.

Table 6.
Results of DSC measurements obtained for nanocomposites based on PP+ZrO_2 and PVDF+ZrO_2.

Samples	$T_{melt.}$ (^{0}C)	$T_{cryst.}$ (^{0}C)	Enthalpy of melting (C/g)	Crystallinity degree (%)
PP	165.09	108.84	91.9	44.8
PP+1%ZrO_2	158.26	112.47	75.92	36.0
PP+3%ZrO_2	157.62	111.52	80.02	38.6
PP+5%ZrO_2	160.24	118.49	76.33	36.8
PVDF	150.39	112.37	40,3	38,3
PVDF+5%ZrO_2	162.67	128.94	48,4	46,1
PVDF+10%ZrO_2	166.01	129.68	46,9	44,6

DSC analysis of nanocomposites showed that the introduction of ZrO_2 nanoparticles into both the PP matrix and PVDF increases the temperature of crystallization of nanocomposites based on them. This once again shows that ZrO_2 nanoparticles are good nucleating particles in the PP and PVDF matrix. It was found that the degree of crystallinity of nanocomposites with the introduction of ZrO_2 nanoparticles into the PP matrix slightly decreases, while in PVDF- it increases. Table 6 shows the results of DSC measurements obtained for nanocomposites based on PP+ZrO_2 and PVDF+ZrO_2.

In fourth chapter Fe_3O_4 magnetite nanoparticles were synthesized and stabilized; the relationship between the structure and

properties of nanocomposites based on ferromagnetic nanoparticles Fe_3O_4 and thermoplastic polymers PP and PVDF were studied. Magnetic Fe_3O_4 nanoparticles were prepared by chemical coprecipitation based on co-precipitation of Fe^{3+} and Fe^{2+} with a molar ratio of 3:2 under an ammonia solution (NH_4OH) as a precipitating agent in a nitrogen atmosphere. Fe_3O_4 nanoparticles were synthesized and stabilized in the presence of 4 stabilizers-surfactants: cetyltrimethylammonium bromide (CTABr), polyethylene glycol (PEG-6000), sodium oleate, and sodium dodecyl sulfate), as well as in the presence of reverse micelles. Figure 21 shows the diffraction pattern of pure magnetic Fe_3O_4 nanoparticles. As can be seen from the figure 21, the main peaks at 30.36^0 (220), 35.68^0 (311), 43.3^0 (400), 57.36^0 (511), and 62.95^0 (440) correspond to magnetite nanoparticles with cubic spinel structure, respectively, database No.00-001-1111.
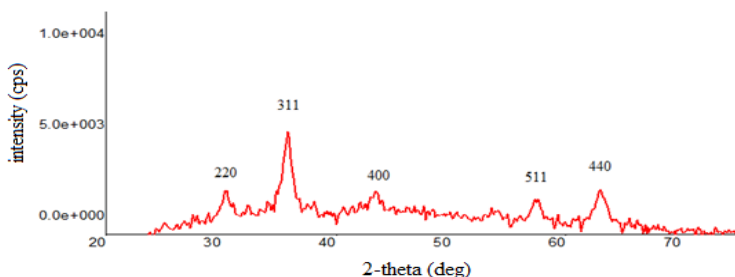
Fig.21. Diffraction pattern of Fe₃O₄ nanoparticles.

Figure 22 shows SEM images of Fe_3O_4 nanoparticles stabilized in the presence of stabilizers - cetyltrimethylammonium bromide (CTABr) (a), polyethylene glycol (PEG) (b), sodium oleate (c), and sodium dodecyl sulfate (d). As can be seen from the figure 22, the average size of Fe_3O_4 nanoparticles in the presence of all 4 surfactants is 5-10 nm. It was revealed that by controlling the conditions of chemical coprecipitation of Fe_3O_4 nanoparticles (the nature and concentration of the surfactant, the concentration of the initial reagents, the ratio of the precursor and the precipitating agent, the pH of the solution (a strong or weak alkali), the method of mixing the components, the type of space-limiting medium (micelle, emulsion, surfactant, etc.) it is possible to obtain homogeneous, monodisperse and pure nanoparticles of magnetite Fe_3O_4.
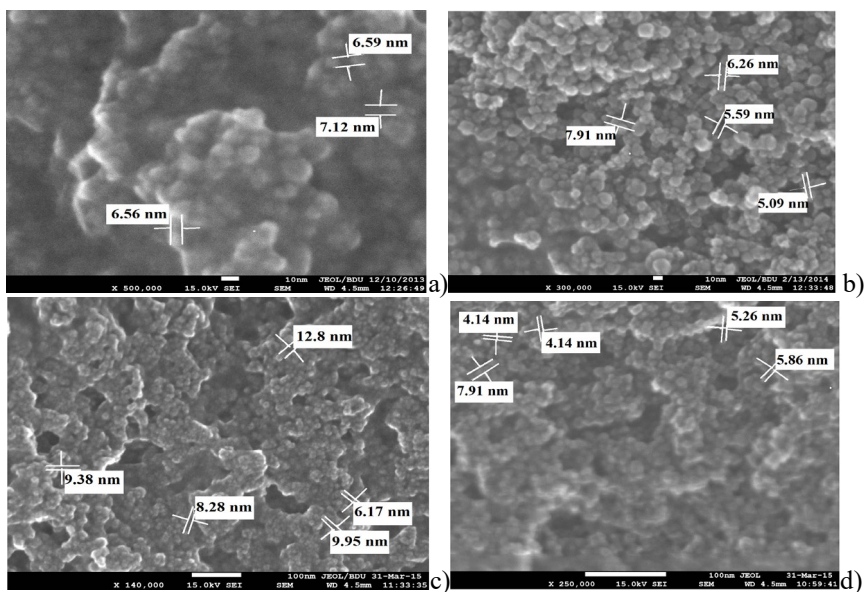
Fig.22. SEM images of Fe₃O₄ nanoparticles stabilized in the presence of CTABr (a), PEG (b), sodium oleate (c) and sodium dodecyl sulfate (d).

In the fourth chapter, the influence of the technological factor on the structure and properties of polymer nanocomposites is also studied. Figure 23 shows SEM images of polymeric nanocomposites based on PP+Fe$_3$O$_4$ obtained by extrusion (a) and hot pressing (b). As can be seen from the figure 23, the distribution of nanoparticles in polymer nanocomposites obtained by extrusion is inhomogeneous and inhomogeneous. At low Fe$_3$O$_4$ contents in the polypropylene matrix, nanoparticles are located between polymer layers in the form of separate clusters; with an increase in the nanoparticle content, the distribution of nanoparticles improves, but at the same time, the number of agglomerated particles in the polymer matrix also increases. The distribution of Fe$_3$O$_4$ nanoparticles in polymer nanocomposites obtained by hot pressing is uniform and monodisperse.
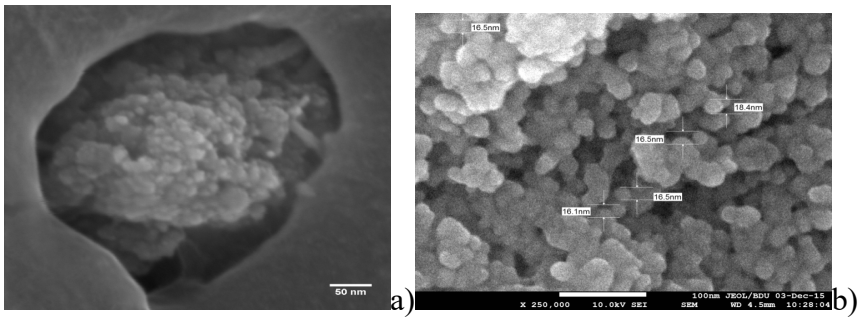
Fig.23. SEM images of PP+Fe₃O₄ nanocomposites obtained by extrusion (a) and hot pressing (b) methods.

Figure 24 shows AFM 2D images of nanocomposites based on PP+10%Fe₃O₄, obtained both by the extrusion method (a) and by the hot pressing method (b). As can be seen from the AFM images, the supramolecular structure of polymer nanocomposites obtained by extrusion and hot pressing methods are different.
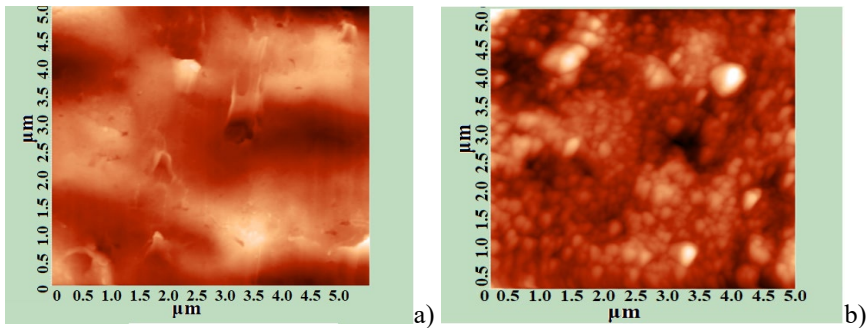

Fig. 24. AFM 2D images of nanocomposites based on PP+10%Fe₃O₄, obtained by extrusion (a) and hot pressing (b) methods.

Figure 25 shows histograms of the surface roughness of nanocomposites based on PP+10%Fe₃O₄, obtained both by the extrusion method and by the hot pressing method. As can be seen from Figure 25, the average roughness for polymer nanocomposites based on PP+10%Fe₃O₄ obtained by the extrusion method is 150-400 nm, and for PP+10%Fe₃O₄ based nanocomposites obtained by hot pressing-40-100 nm. This pattern is observed for almost all contents

of magnetite nanoparticles in the polypropylene matrix. As can be seen from AFM images and histograms of surface roughness of nanocomposites, the supramolecular structure of nanocomposites obtained by hot pressing is more ordered than for nanocomposites obtained by extrusion method.
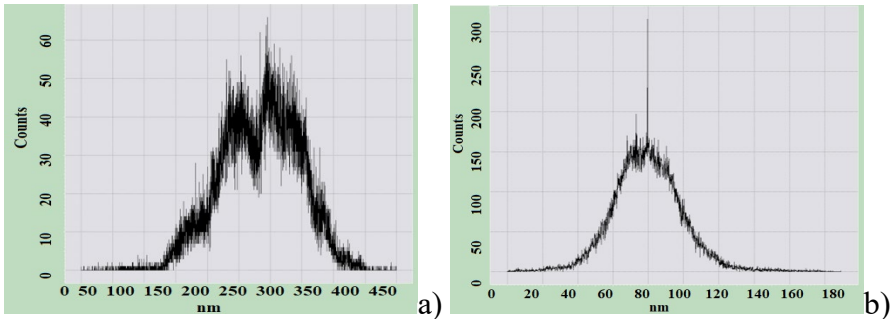

Fig. 25. Histogram of the surface roughness of nanocompositions based on PP+10%Fe$_3$O$_4$, obtained by extrusion (a) and hot pressing (b) methods.

Figure 26 shows the dependences of tensile stress on deformation for nanocomposites based on PP+Fe$_3$O$_4$, obtained by extrusion (a) and hot pressing (b) methods. The compression stress-strain curves of nanocomposites were obtained using a Zwick/Roell Z010 equipment (Zwick/Roell GmbH, Germany). To determine the elasticity and Young's modulus, specimens cut in a certain shape were stretched under a force of 1 kN at a rate of 10 mm/min.The results of tensile tests for nanocomposites show that the introduction of Fe$_3$O$_4$ nanoparticles into the polymer by both the extrusion and the hot pressing methods caused a decrease in the elongation at break of the nanocomposites in comparison with the pure matrix. For nanocomposites obtained by extrusion, the decrease in elongation at break is sharper. This is due to the presence of several agglomerated nanoparticles in the PP due to the extrusion process. However, when Fe$_3$O$_4$ nanoparticles are introduced into a polymer matrix, both by hot pressing and extrusion methods, nanocomposites still exhibit high plastic deformation.
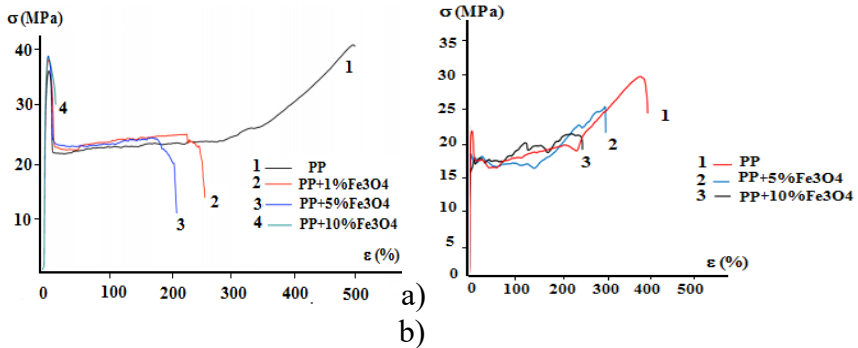
Fig.26. Deformation curves of compression of samples of nanocomposite films based on PP+Fe₃O₄, obtained by extrusion (a) and hot pressing (b) methods.

Fig.27 shows the dependence of the magnetic moment on temperature m (T) at a magnetic field induction of 0.1 Tesla for a nanocomposite based on PP+10%Fe₃O₄, obtained by hot pressing (a) and extrusion (b) methods.
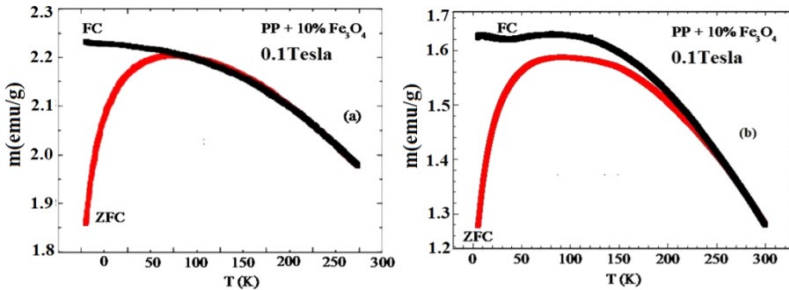

Fig.27. Dependence of the magnetic moment of the nanocomposite based on PP+10%Fe₃O₄, obtained by hot pressing (a) and extrusion (b) methods, on temperature at a magnetic field induction of 0.1 Tesla.

The m(T) measurements of magnetic moment as function of the temperature were performed in Zero Field Cooling (ZFC)-Field Cooling (FC) conditions. More precisely, the sample was first cooled down to 5 K in absence of field, then the field was switched on at 0.1 Tesla and the data were acquired for increasing temperature (ZFC) up to the room temperature 300 K. After that, the sample was cooled down again and FC magnetic moment was acquired in presence of field. As can be seen from Fig.27 the blocking temperature for the

polymer nanocomposite based on PP+10%Fe$_3$O$_4$ obtained by hot pressing method is 90 K, and for the nanocomposite obtained by extrusion method it is 200 K, i.e. nanocomposites obtained by hot pressing retain their magnetic properties even at low temperatures, and by extrusion only at room temperature. Figure 28 shows the dependences of the specific magnetization of the nanocomposite based on PP+10% Fe$_3$O$_4$, obtained by hot pressing (a) and extrusion (b) methods, depending on the intensity of the magnetic field.
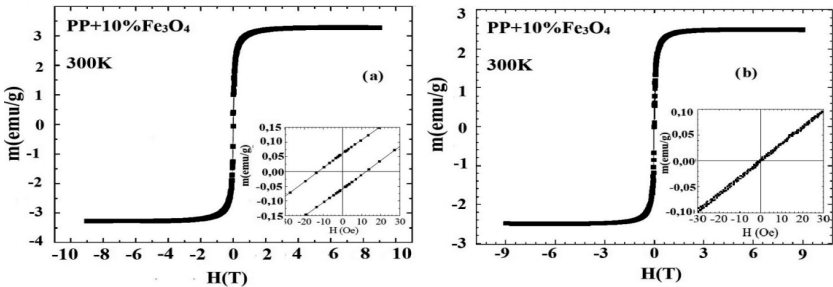

Fig.28. Dependence of the specific magnetization of the nanocomposite based on PP+10%Fe$_3$O$_4$, obtained by hot pressing (a) and extrusion (b) methods, on the magnetic field intensity at a temperature of T=300 K.

It can be seen that an increase in the value of the specific magnetization of the nanocomposites is observed with an increase in the magnetic field. It was found that with an increase in the magnetic field strength for a nanocomposite based on PP+10%Fe$_3$O$_4$ obtained by hot pressing method, the magnetization increases to 3 emu/g, and then saturation is observed. For a nanocomposite based on PP+10%Fe$_3$O$_4$, obtained by extrusion method, the specific magnetization increases to 2.5 emu/g, and then saturation is observed. For all nanocomposites obtained both by the extrusion and hot pressing methods, hysteresis is not observed, which proves the superparamagnetic behavior of these nanocomposites. It has been established that the main advantage of composites obtained by hot pressing over other methods of preparation is determined by the homogeneous distribution of the filler in the polymer matrix and the

defect-free structure. Furthermore, the supramolecular structure of polymer nanocomposites obtained by hot pressing can be varied over a wide range, and various magnetic anisotropy can be achieved. This makes it possible to create magnetic nanocomposite structures with distinctive magnetic properties.
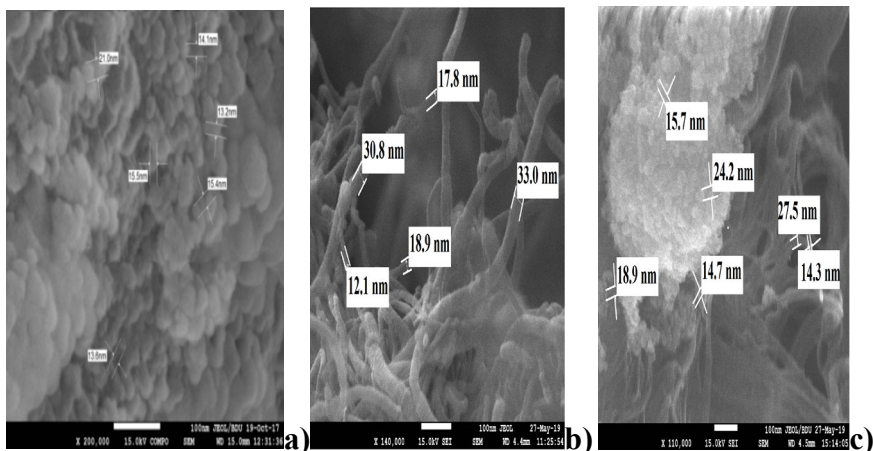

Fig.29. SEM images of polymer nanocomposites based on PVDF+Fe$_3$O$_4$ (a), PVDF+MWCNTs (b) and PVDF+Fe$_3$O$_4$+MWCNTs (c).

In addition three-component polymer nanocomposites based on PVDF, magnetite nanoparticles (Fe$_3$O$_4$) and multi-walled carbon nanotubes (MWCNTs) were investigated in the dissertation work. Figure 29 shows SEM images of polymer nanocomposites based on PVDF+Fe$_3$O$_4$ (a), PVDF+MWCNTs (b) and PVDF+Fe$_3$O$_4$+MWCNTs (c). Actually, no increase in the size of both magnetite nanoparticles and carbon nanotubes was observed during the formation of a three-phase nanocomposite based on PVDF+Fe$_3$O$_4$+MWCNTs. Thus, the average diameter of carbon nanotubes in the case of two-component PVDF+MWCNT and three-component nanocomposite PVDF+ Fe$_3$O$_4$+ MWCNT is 12-30 nm. The electrical properties of three-phase polymer nanocomposites based on PVDF+Fe$_3$O$_4$+ MWCNTs have been studied. Measurement of the dielectric permittivity and dielectric loss tangent was

conducted using immittance meter MNIPI E7-20 by applying a broadband meter E7-20 immittance. Fig.30 shows the dependences of the dielectric constant (a) and the tangent of the dielectric loss angle (b) for polymer nanocomposites based on PVDF+Fe$_3$O$_4$+MWCNTs depending on the frequency.
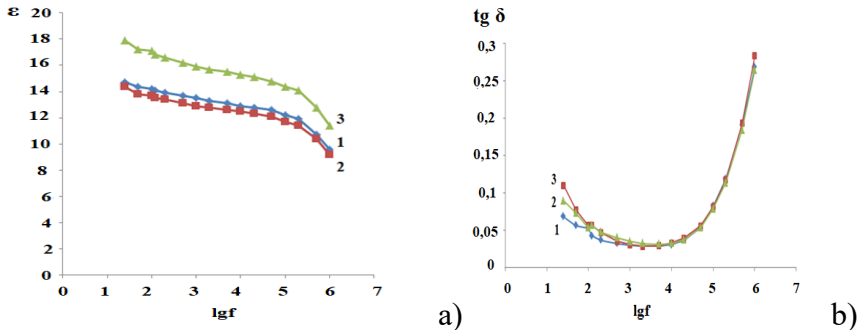

a)   b)

Fig.30. Dependences of dielectric constant (a) and dielectric loss tangent (b) for polymer nanocomposites based on PVDF+Fe$_3$O$_4$+MWCNTs depending on frequency: 1. PVDF+5%Fe$_3$O$_4$+5%MWCNTs;2.PVDF+5%Fe$_3$O$_4$+10%MWCNTs;3.PVDF+5%Fe$_3$O$_4$+15%MWCNTs.

As can be seen from Fig.30 (a), the dielectric constant of nanocomposites based on PVDF+Fe$_3$O$_4$+MWCNTs sharply decreases depending on the frequency. This is explained by the deterioration of polarization processes in nanocomposites with increasing frequency. Fig.30 (b) that the dielectric loss tangent of nanocomposites decreases to 1 kHz, and after 1 kHz, an increase in dielectric losses of nanocomposites based on PVDF+Fe$_3$O$_4$+MWCNTs is observed. An increase in dielectric losses of nanocomposites at high frequencies shows an increase in energy dissipation at high frequencies. From this dependence, it can be concluded that these three-phase nanocomposites can be promisingly used as radio-absorbing nanocomposites in a wide frequency range.

Fig.31 shows the values of the absorption coefficient of electromagnetic waves for nanocomposites PVDF+Fe$_3$O$_4$ (1), PVDF+MWCNTs (2) and PVDF+5%Fe$_3$O$_4$+10%MWCNTs (3).
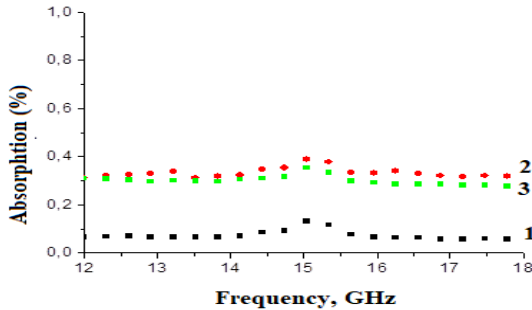
Fig.31. The absorption coefficient of electromagnetic waves by composites based on PVDF+40%Fe₃O₄ (1), PVDF+20%MWCNTs (2), PVDF+5%Fe₃O₄+10%MWCNTs (3).

Analysis of the absorption spectra as a function of frequency shows that the maximum values of the absorption coefficient are observed for composites containing 20% MWCNTs in a PVDF matrix. Very close absorption values are observed for three-phase nanocomposites containing PVDF+5%Fe₃O₄+10%MWCNTs. An increase in the absorptive capacity of magnetic nanocomposites at radio frequency wavelengths can be explained by the fact that with an increase in the concentration of magnetic nanoparticles, the value of the magnetic permeability and the dielectric loss tangent of nan composites increases, and this leads to an increase in the loss of electromagnetic energy at high frequencies, which leads to an increase in the absorption of electromagnetic waves. Therefore, it can be concluded that the combination of electrically conductive and magnetic inclusions makes it possible to obtain materials with high absorption of ultra-frequency electromagnetic waves and, at the same time, to save expensive multi-walled carbon nanotubes.

In the **fifth chapter**, the optical, photoluminescent, and dielectric properties of nanocomposites based on thermoplastic polyar PVDF and non-polar PP polymers and semiconducting nanoparticles of metal sulfides CdS, PbS and ZnS are investigated. PbS, ZnS, and CdS nanoparticles were stabilized in the presence of the surfactant CTABr by chemical precipitation from colloidal solutions of the corresponding precursors of cadmium chloride, zinc chloride, and lead acetate salts. Sodium sulfide Na₂S×9H₂O was

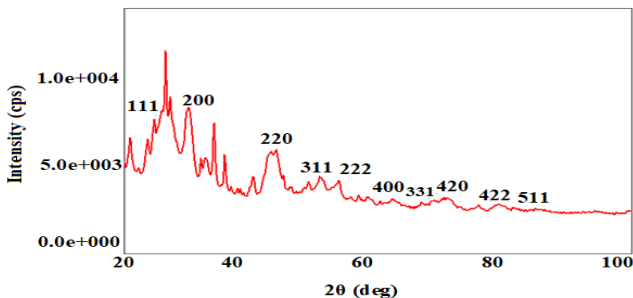taken as a precipitating agent. Figure 32 shows is a diffraction pattern of lead sulfide nanoparticles.

Fig. 32. Diffraction pattern of lead sulfide (PbS) nanoparticles.

As you can see, the main peaks in the diffractogram at 2θ equal to 26.78^0 (111); 30.11^0 (200); 43.37^0 (220); 51.1^0 (311); 53.97^0 (222); 62.54^0 (400); 68.63^0 (331); 71.0^0 (420); 79.38^0 (422) and 85.19^0 (511) belong to galena-type lead sulfide nanoparticles. PbS crystallizes in a B1 (NaCl) type cubic lattice with the Fm3m space group with crystal lattice parameters of 0.594 nm, 0.5936 nm and 0.5929 nm according to the ICCD PDF database (00-210-4270). Figure 33 (a) and (b) shows the diffraction pattern of cadmium sulfide nanoparticles.

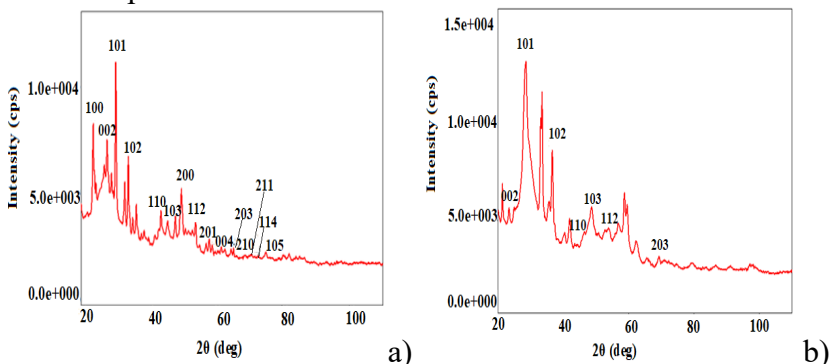**Fig. 33. Diffraction patterns of cadmium sulfide CdS (a) and zinc ZnS (b) nanoparticles.**

Peaks observed on the X-ray diffraction pattern at 2θ equal 24.9^0 (002); 26.6^0 (101); 28.3^0 (102); 36.8^0 (110); 43.9^0 (103); 48.1^0 (200); 51.1^0 (112); 52.1^0 (201); 53.1^0 (004); 67.1^0 (203); 69.6^0 (210); 71.2^0 (211); 72.8^0 (114) and 75.9^0 (105), belong to the hexagonal structure

of CdS of the wurtzite type, with crystal lattice parameters 4.16, 4.16 and 6.77 A^0 in accordance with Card ICCD PDF 00-101-1054, inherent in the stable state of cadmium sulfide. As can be seen, the main peaks in the diffractogram 33 (b) at 2θ are equal to 28.5^0 (002), 30.5^0 (101), 39.5^0 (102), 47.5^0 (110), 51.5^0 (103), 56.5^0 (112), and 73.0^0 (203) belong to nanoparticles of zinc sulfide with hexagonal crystal lattice of the wurtzite type according to the ICCD PDF database (00-101-1195).

Figure 34 shows SEM images of PbS (a), CdS (b), and ZnS (c) nanoparticles stabilized in the presence of CTABr. As can be seen from SEM images, the average size of stablizied PbS nanoparticles is 7-13 nm, CdS nanoparticles - 5-10 nm, and ZnS nanoparticles - 3-5 nm.
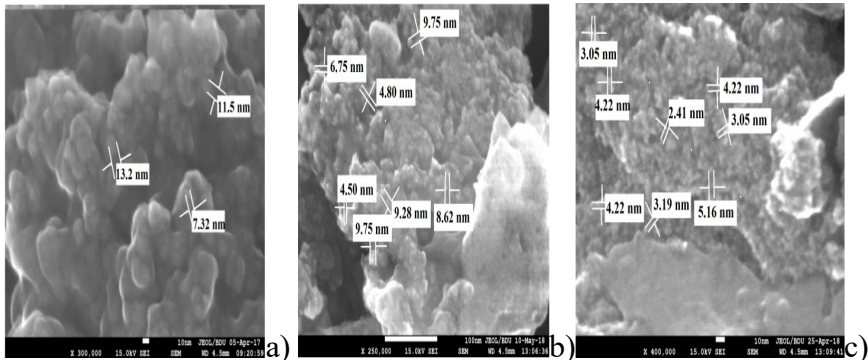
Fig. 34. SEM images of PbS (a), CdS (b) and ZnS (c) nanoparticles stabilized in the presence of CTABr.

Figure 35 shows a plot of the frequency dependence of the dielectric constant of PP+PbS-based nanocomposites. As can be seen from the graph, with the introduction of PbS nanoparticles into PP, dielectric constant of nanocomposites increases to 3% and then decreases. It is also seen from Fig.35 (a) that dielectric constant ε does not change depending on the frequency at all concentrations, and only at high frequencies does the dielectric constant decrease. A decrease in dielectric constant ε at high frequencies is associated with deterioration in polarization processes.

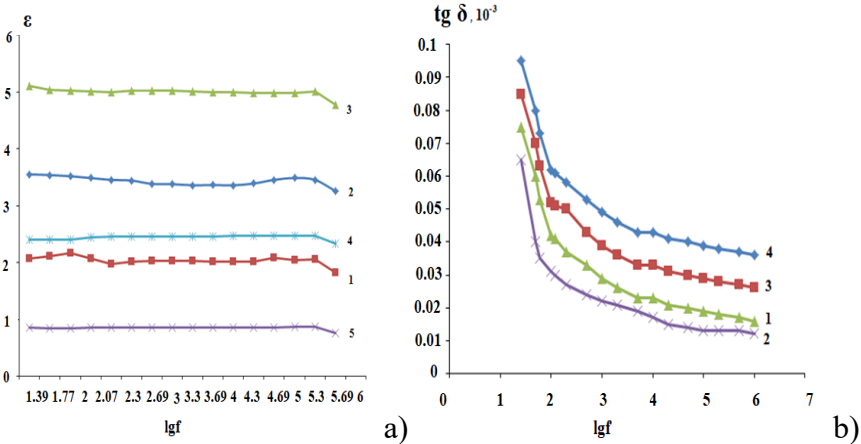**Fig.35. Dependence of the dielectric constant (a) and dielectric loss tangent (b) of nanocomposites on the frequency: a) 1.PP;2.PP+1%PbS; 3.PP+3%PbS;4.PP+5%PbS; 5.PP+10%PbS; b) 1.PP; 2. PP+3%PbS; 3. PP+5%PbS; 4. PP+10%PbS.**

Figure 35 (b) shows the dependence of tg δ of nanocomposites on frequency and it can be seen that dielectric loss tg δ decreases depending on the frequency; however, at high frequencies the rate of decrease in tgδ decreases. The maximum value of dielectric constant ε and the minimum value of dielectric loss tangent tg δ at 3% concentration of PbS nanoparticles is explained by the fact that at a given content, PbS nanoparticles play the role of a crystallization center in the polymer matrix. A decrease in dielectric loss tangent tg δ with the introduction of PbS nanoparticles into the polymer matrix is associated with the formation of a more optimal structure and with the fact that PbS nanoparticles behave as a structural in the PP polymer matrix. Figure 36 shows the temperature dependence of the resistivity of PP+PbS-based nanocomposites and it can be seen that for PP+PbS-based nanocomposites ρ changes abruptly as a function of temperature for a small temperature range, i.e., a posistor effect is observed. The sharp change in resistance depending on temperature is explained by an increase in the distance between nanoparticles due to the destruction of the crystalline phase of the polymer matrix.
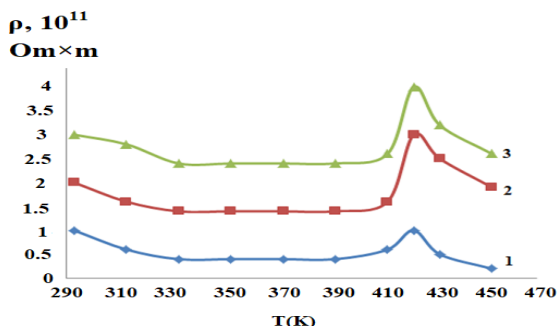
Fig.36. Dependence of the resistivity of nanocomposites on temperature: 1. PP+1%PbS; 2. PP+3%PbS; 3. PP+10%PbS.

Were studied the photoluminescent properties of PP+PbS-based nanocomposites depending on the concentration of PbS nanoparticles. It was found that the photoluminescence intensity increases with an increase in the concentration of PbS nanoparticles to 3%, and then decreases. It is known that bulk lead sulfide PbS shows photoluminescence in the infrared region in the wavelength range 1000-1200 nm. With a decrease in the size of PbS nanoparticles, in polymer nanocomposites based on PP+PbS due to quantum size effects, the photoluminescence peak shifts from the far infrared region to the near infrared region and is observed at 765 nm.

In the fifth chapter, hybrid polymer nanocomposites based on PP+CdS/ZnS, PVDF+CdS/ZnS, PP+PbS/CdS and PVDF+PbS/CdS were also obtained and studied for the first time.

Figures 37 shows SEM images of hybrid nanocomposites based on PP+CdS/ZnS depending on the concentration of ZnS and CdS nanoparticles. SEM images show that ZnS and CdS nanoparticles are equally uniformly distributed within the polymer matrix. It was found that with an increase in the concentration of nanoparticles, the average size of nanoparticles of both zinc sulfide and cadmium sulfide in polymer matrix increases. The average nanoparticle size for a hybrid nanocomposite based on PP+3%CdS/ZnS is 40-54 nm, for PP+5%CdS/ZnS−29-56 nm. It was also found that CdS and ZnS nanoparticles are distributed in the polymer matrix in the form of separate dispersed phases.
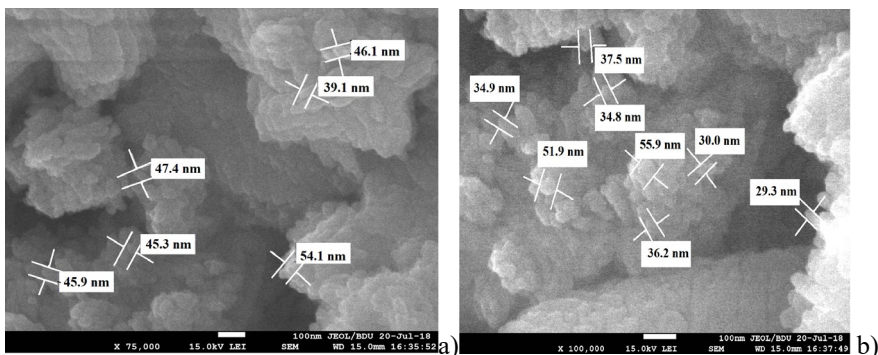
Fig.37. SEM images of hybrid nanocomposites based on PP+CdS/ZnS depending on the concentration of ZnS and CdS nanoparticles: a) PP+3%CdS/ZnS; b) PP+5%CdS/ZnS.

The absorption spectra of hybrid nanocomposites based on PP+CdS/ZnS were studied by ultraviolet (UV) spectroscopy. The absorption spectra of nanocomposites were studied on a Specord 250 Plus spectrophotometer at room temperature at a wavelength of 200-600 nm. The energy gap of the nanocomposites was calculated from the absorption spectra by extrapolation. Were studied the UV absorption spectra and the optical absorption edge for nanocomposites based on PP+ZnS, PP+CdS, and PP+CdS/ZnS. It was found that for nanocomposites based on PP+ZnS, the band gap is 3.65 eV, for PP+CdS, 2.8 eV and for PP+CdS/ZnS nanocomposite, 4.6 eV. Fig.38 shows the absorption UV spectra (a) and the optical absorption edge (b) for hybrid nanocomposites based on PP+CdS/ZnS depending on the concentration of ZnS and CdS nanoparticles. It was found that the band gap for PP+CdS/ZnS hybrid nanocomposites decreases with an increase in the content of ZnS and CdS nanoparticles in the polymer matrix. Thus, for a hybrid nanocomposite based on PP+1%CdS/ZnS, the band gap is 5.2 eV; for a nanocomposite based on PP+3%CdS/ZnS and PP+5%CdS/ZnS - 5.1 eV, and for a nanocomposite based on PP+10%CdS/ZnS - 4.6 eV. The decrease in the band gap of nanocomposites is explained by the increase and agglomeration of nanoparticles depending on the content of CdS and ZnS nanoparticles.
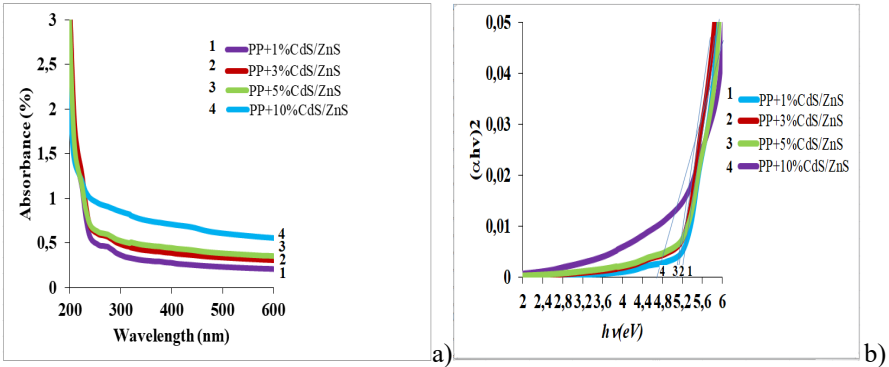
Fig.38. Absorption UV spectra (a) and optical absorption edge (b) for hybrid nanocomposites based on PP+CdS/ZnS depending on the concentration of CdS and ZnS nanoparticles: 1. PP+1%CdS/ZnS, 2. PP+3%CdS/ZnS, 3. PP+5%CdS/ZnS, 4. PP+10%CdS/ZnS.

Figure 39 shows the photoluminescence spectra of nanocomposites based on PP+CdS (a), PP+ZnS (b) and PP+CdS/ZnS (c). The photoluminescence spectra for the PP+CdS nanocomposite were studied upon excitation with light with a wavelength of 398 nm, the photoluminescence spectra for the nanocomposite based on PP+ZnS- upon excitation with light at a wavelength of 260 nm, and the photoluminescence spectra for the hybrid nanocomposite based on PP+CdS/ZnS- at excitation by light with a wavelength of 260 nm. As can be seen from Figure 39 (a), the peaks at 446 nm, 458 nm, 465 nm, 517 nm, 528 nm, 542 nm, 567 nm and 573 nm belong to CdS nanoparticles. For single-crystal CdS, the emission during interband recombination has a wavelength of 517 nm. A blue shift is observed for CdS quantum dots; reduction of the emission wavelength. The main peaks observed in Fig.39 (b) belongs to zinc sulfide nanoparticles. As can be seen from Fig. 39 (c), at 1% content of CdS and ZnS nanoparticles, the photoluminescence intensity is maximum; with a further increase in the content of nanoparticles, the photoluminescence intensity decreases.
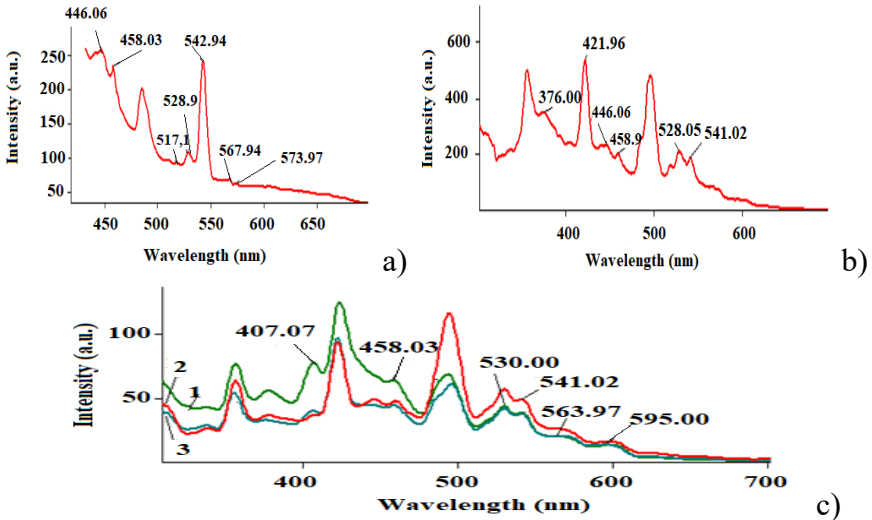
Fig.39. Photoluminescence spectrum of nanocomposites based on PP+CdS (a), PP+ZnS (b), and PP+CdS/ZnS (c) (1.PP+1%CdS/ZnS, 2. PP+5%CdS/ZnS, 3. PP+10%CdS/ZnS).

This is explained by the fact that with an increase in the concentration of nanoparticles, their size increases and the specific surface area decreases, and this leads to a decrease in the contact area between the polymer and the nanoparticle. A decrease in the interface leads to a decrease in interphase interactions, and this, in turn, to a change in the photoluminescence intensity. From the photoluminescence spectra data, it can be concluded that upon obtaining hybrid nanocomposites, such as PP+CdS/ZnS, the spectrally sensitive region of the spectrum broadens. Consequently, it was found that hybrid nanocomposites, first developed in the dissertation work, can luminesce at a wide wavelength range, which makes it possible to use these nanocomposites in various fields, including as active elements of solar cells, displays, converters, etc.

Besides, the photosensitivity of hybrid nanocomposite films based on PVDF+CdS/ZnS was discovered for the first time in the dissertation work. Have been established that, nanocomposites with 3, 5 and 10% by weight of CdS and ZnS nanoparticles exhibit photosensitivity in the wavelength range of 330-590 nm. Regardless

of the content of nanoparticles, the short and long wavelength parts of the spectrum exhibit maxima corresponding to the band gap of CdS and ZnS nanoparticles. The presence of both maxima indicates that the CdS and ZnS nanoparticles do not form a solid solution in the PVDF matrix. For the PVDF+3%CdS/ZnS nanocomposite photosensitivity is observed at a wavelength of 340 nm and 504 nm, while for the PVDF+10%CdS/ZnS nanocomposite photosensitivity is observed at 345 nm and 494.7 nm. Have been determined that with an increase in the content of nanoparticles, the intensity of the maximum characteristic of CdS increases, and the intensity of the maximum for ZnS decreases. That is, with an increase in the content of nanoparticles upon absorption of light, the dominant role is played by CdS nanoparticles. This is explained by the fact that with an increase in the content of nanoparticles, the resistivity of CdS and ZnS nanoparticles associated with light scattering decreases.

The sixth chapter is devoted to studying the possibilities of using polymer nanocomposites based on thermoplastic polymers PP and PVDF and nanoparticles of metals, metal oxides, and sulfides. New electret polymer nanocomposites based on PP, PVDF, and ZrO_2 nanoparticles (PP+ZrO_2 and PVDF+ZrO_2), TiO_2 (PP+TiO_2 and PVDF+TiO_2), developed in the dissertation work, showed an electret effect, which is noticeably superior in its characteristics to the known traditional analogs, which makes it possible to apply these nanocomposites to obtain high-performance electret microphones, electroacoustic devices, etc. It was found that the lifetime of electret charges for polymer nanocomposites based on PVDF+TiO_2 is 485 days; for nanocomposites based on PP+TiO_2 -321 days; for PP+ZrO_2 - 225 days, and PVDF+ZrO_2 - 257 days.

The polymer nanocomposites developed in the dissertation work based on thermoplastic polymers and superparamagnetic magnetite nanoparticles were tested for the absorption of electromagnetic waves (EMW) in the high frequency range of 0.1-30 GHz. Table 7 shows the results of absorption of high-frequency electromagnetic waves (EMW) (0.1-30 GHz) by magnetic nanocomposites based on PP+Fe_3O_4 and PVDF+Fe_3O_4.

№	Samples	% Fe$_3$O$_4$	Thick ness (μm)	I$_0$ (μA)	I (μA)	EMW absorption (%)
1	PP+Fe$_3$O$_4$	5	400	260	220	15
3	PP+Fe$_3$O$_4$	10	400	275	233	16
4	PP+Fe$_3$O$_4$	20	400	275	230	17
5	PP+Fe$_3$O$_4$	40	400	275	213	23
6	PVDF+Fe$_3$O$_4$	5	500	260	245	6
7	PVDF+Fe$_3$O$_4$	10	500	260	232	11
8	PVDF+Fe$_3$O$_4$	20	500	260	172	34
9	PVDF+Fe$_3$O$_4$	40	500	260	168	36
10	PVDF+Fe$_3$O$_4$	40	1100	260	148	43
11	PVDF+Fe$_3$O$_4$	40	1668	260	101	62

As can be seen, with an increase in the concentration of Fe$_3$O$_4$ nanoparticles in PP and PVDF polymers, the absorption of electromagnetic waves increases. Thus, at a content of 5% Fe$_3$O$_4$ in PP, the absorption of electromagnetic waves is 15%; at 10% content -16%; at 20% content - 17%; at 40% is 23%. As can be seen from Table 7, in a nanocomposite based on PVDF+5%Fe$_3$O$_4$ with a sample thickness of 500 μm, the absorption of electromagnetic waves is 6%; in PVDF+10%Fe$_3$O$_4$ with a sample thickness of 500 microns - 11%; in PVDF+20%Fe$_3$O$_4$ with a sample thickness of 500 microns - 34%; in PVDF+40%Fe$_3$O$_4$ with a sample thickness of 500 μm - 36%. With an increase in the thickness of the samples, a sharp increase in the absorption of electromagnetic waves was observed. For a nanocomposite based on PVDF+40%Fe$_3$O$_4$ with a sample thickness of 1100 μm (1,1 mm), the absorption of electromagnetic waves is 43%, and with a sample thickness of 1668 μm (1,668 mm), 62%. Thus, it has been found that polymer magnetic nanocomposite materials based on thermoplastic polymers PP and PVDF and Fe$_3$O$_4$ nanoparticles are capable of absorbing electromagnetic in the

frequency range 0.1-30 GHz. This is explained by the fact that Fe_3O_4 nanoparticles are single-domain particles and exhibit superparamagnetic properties, and as a result of induction processes, easily turning around, they create an alternating magnetic field around them when high-frequency electromagnetic waves hit them. As a result, electromagnetic waves lose their energy and are absorbed. Also, with an increase in the concentration of magnetic Fe_3O_4 nanoparticles, the value of the magnetic permeability and dielectric loss tangent of the nanocomposites increases, and this leads to an increase in the loss of electromagnetic energy at high frequencies and, as a result, the absorption capacity of magnetic nanocomposites at radio frequency wavelengths increases. Thus, these results indicate that these polymer nanocomposites can be successfully applied in the military and defense industry if thin nanocomposite coatings are developed on their basis, which will absorb electromagnetic waves and make objects invisible.

Also in the dissertation work, it was found that nanocomposites based on $PP+Fe_3O_4$ based nanocomposites obtained by hot pressing method absorb ultra-frequency electromagnetic waves (0.1-30 GHz) better than composites obtained by extrusion method (Table 8). This is because that the electromagnetic waves freely pass through the defects of composites obtained by the extrusion method. At the same time, the supramolecular structure of polymer nanocomposites obtained by hot pressing method can be varied over a wide range, and various magnetic anisotropy can be achieved. And this creates the possibility of creating magnetic nanocomposite structures with distinctive magnetic properties.

It was also revealed that the polymer nanocomposites based on $PP+Fe_3O_4$ and $PVDF+Fe_3O_4$, developed in the thesis, exhibit a magnetoresistive effect. Due to this effect, it is possible to use these magnetic polymer nanocomposites to create various devices and equipment for magnetic recording. It is also possible to use these polymer nanocomposites to develop highly sensitive magnetic field sensors that can respond to even small changes in the magnetic field.

Table 8.

Results of absorption of high-frequency electromagnetic waves by magnetic polymer based on PP+Fe₃O₄, obtained by hot pressing and extrusion.

№	Samples	Thickness (μm)	I_0 (μA)	I (μA)	EMW absorption (%)
1	PP+10%Fe$_3$O$_4$ (hot pressing method)	400	275	235	16
2	PP+20%Fe$_3$O$_4$ (hot pressing method)	400	275	230	17
3	PP+40%Fe$_3$O$_4$ (hot pressing method)	400	275	213	23
4	PP+10%Fe$_3$O$_4$ (extrusion method)	400	270	254	6
5	PP+20%Fe$_3$O$_4$ (extrusion method)	400	270	244	10
6	PP+40%Fe$_3$O$_4$ (extrusion method)	400	270	232	14

It was also found that the hybrid nanocomposites developed in the dissertation work based on semiconductor nanoparticles PbS, ZnS and CdS can luminesce at a wide wavelength range, which makes it possible to use these nanocomposites in various fields, including as active elements of solar cells, displays, converters, etc. Also, the high photosensitivity of these hybrid nanocomposites can make it possible to successfully use them as elastic photoresistors.

CONCLUSION

1. Were synthesized nanoparticles of metals of cobalt, nickel, iron, copper, iron oxide Fe_3O_4, metal sulfides CdS, PbS and ZnS. It has been established that by varying the conditions of chemical deposition: the nature of the surfactant, the concentration of the surfactant, the concentration of the initial reagents, the temperature, the method of mixing the components, the type of space-limiting medium (micelle, emulsion, surfactant, etc.), one can vary the dispersion, homogeneity, dimension, and purity of the obtained nanoparticles [11,17,18,20,39,44,50,57,62].

2. It has been established that the introduction of nanosized metallic fillers at low contents of PP and PVDF polymers in the matrix leads to an improvement in the thermophysical, electrical, mechanical, and strength properties of polymer nanocomposites formed on their basis. This is explained by the fact that at low contents of metal nanoparticles in the polymer matrix, nanocomposites with a more perfect supramolecular structure are formed, i.e. at low contents in the polymer matrix, nanoparticles of metals, oxides and sulfides of metals play the role of a nucleus and structure-forming agent [37,38,44,61,62].

3. It has been shown that for nanocomposites based on $PP+ZrO_2$ after polarization under the influence of a corona discharge, the root-mean-square roughness of the sample surface for unpolarized samples is 60-120 nm, and for polarized ones, it is 30-60 nm, that is, under the influence of polarization, the structural elements are refined. It was also found that after polarization under the influence of a corona discharge, the photoluminescence intensity of the nanocomposite increases, and the increase in intensity depends on the concentration of nanoparticles in the matrix. It is shown that in the course of a corona discharge due to migration polarization at the interface between the components of the $PP+ZrO_2$ nanocomposite, a sufficiently large number of electric charges are accumulated, and these charges create a high internal local field and, under the influence of this field, additional luminescent centers are excited in the nanocomposites, as a result of which after polarization, the

luminescence intensity increases [19,28,52,70].

4. It was found that for nanocomposites based on PP+ZrO$_2$, PVDF+ZrO$_2$, PP+PbS, a posistor effect is observed; in the region of the temperature of the destruction of the crystalline phases of polymers, the resistivity of nanocomposites changes abruptly with an extremum. In our opinion, this is because the destruction of the crystalline phases of polymers increases the distance between nanoparticles, which in turn leads to a sharp increase in the resistance of nanocomposites [8,9,17,18].

5. It is shown that the change in the electret and photoluminescent properties of nanocomposites based on PP+TiO$_2$ and PVDF+TiO$_2$, depending on the polarization conditions, is associated with a change in the conditions of charge stabilization and on the degree of interaction between the phases and the thickness of the boundary layer [27, 28, 70].

6. It was found that the introduction of nanoparticles of metals and metal oxides (Cu, Fe, ZrO$_2$ and Fe$_3$O$_4$) into polymer matrice PP up to 1-5% content increases the thermal stability of nanocomposites, and a further increase in the content of nanoparticles decreases the thermal stability of nanocomposites. An increase in the thermal stability of nanocomposites to 1-5% of the content of nanoparticles is due to the fact that, up to this concentration, nanoparticles play the role of a structurant in polymer matrices, and then as a filler [16,31,34,37,71].

7. The influence of the technological factor on the structure and properties of magnetic polymer nanocomposites based on PP+Fe$_3$O$_4$ has been investigated and it has been established that nanocomposites obtained by hot pressing method in comparison with extrusion method are determined by a more homogeneous distribution of the filler in the polymer matrix and a defect-free structure. At the same time, there is a great possibility of varying the supramolecular structure of polymers obtained by hot pressing method, which makes it possible to obtain nanocomposites with different magnetic anisotropy [45,64].

8. It was found that with an increase in the concentration of Cu, Fe, ZrO$_2$, Fe$_3$O$_4$ nanoparticles in PP and PVDF polymer matrices, the

crystallization temperature of nanocomposites shifts to high temperatures, which is due to the fact that nanoparticles play the role of a nucleating agent for the formation of the supramolecular structure of the polymer, which results in crystallization maxima shift towards high temperatures [16,31,34,37,71].

9. It has been experimentally established that magnetic polymer nanocomposites based on PP, PVDF, and Fe_3O_4 nanoparticles exhibit a magnetoresistive effect, i.e. under the action of an external magnetic field, the electrical resistance of the nanocomposites changes sharply, which can be explained by the mutual orientation of the magnetic moments of the superparamagnetic Fe_3O_4 nanoparticles, which lead to the tunneling of charge carriers and a change in the resistance of the nan composites [54].

10. It has been shown that magnetic polymer nanocomposites based on PP, PVDF and Fe_3O_4 nanoparticles have the ability to high frequency electromagnetic waves in the wave frequency range 0.1-30 GHz. It was found that with an increase in the concentration of magnetic Fe_3O_4 nanoparticles, the value of the magnetic permeability and dielectric loss tangent of nanocomposites increases, which leads to an increase in the losses of electromagnetic energy at high frequencies. It was also revealed that nanocomposites obtained by hot pressing method absorb electromagnetic waves better than nanocomposites obtained by extrusion method. This is due to the fact that electromagnetic waves can freely pass through the defects of composites obtained by the extrusion method [53,56].

11. New hybrid photoluminescent polymer nanocomposites based on PP+CdS/ZnS and PVDF+CdS/ZnS have been obtained and it has been shown that by varying the concentration of individual components of semiconductor clusters, one can vary the spectrally sensitive luminescence region [47,51,63,67,68,69].

12. Three-component radio-absorbing composite materials based on polyvinylidene fluoride with ferromagnetic nanoparticles of iron oxides and multi-walled carbon nanotubes (MWCNTs) have been obtained and it is shown that high absorptions are observed in three-phase nanocomposites containing $PVDF+5\%Fe_3O_4+10\%MWCNTs$. Thus, it can be concluded that the combination of electrically

conductive and magnetic inclusions makes it possible to obtain materials with high absorption and, at the same time, to save on expensive MWCNTs [59, 72].

Published scientific works on the topic of the dissertation

1. Magerramov, A.M. The effect of the temperature-time mode of crystallization on the morphology and properties of nanocomposites based on polypropylene and cadmium sulfide / M.A.Ramazanov, F.V.Gadzhieva, S.G.Alieva // J.Surface Engineering and Applied Electrochemistry, -2011. 47,-p.428-432.

2. Maharramov, A.M. Photoluminescent properties of nanocomposites based on PVDF+CdS and PP+ CdS / A.M.Magerramov, M.A.Ramazanov, F.V.Hajiyeva // Journal of Applied Physics, -2011. №3,- p.107-109.

3. Maharramov, A.M. Formation of nanoporous structures of polypropylene irradiated by high energy heavy ions / A.M.Maharramov, M.A.Ramazanov, F.V.Hajiyeva, S.Q.Aliyeva // J. Nanomedicine & Nanotechology,- 2012. 3(5), -p. 1000141.

4. Hajiyeva, F.V., Gulieva V.M. SEM analysis of nanocompositions based on polymer and nanoparticles of zirconium dioxide // Materials of the VII Republican Scientific Conference "Actual Problems of Physics", Baku, Azerbaijan: - November 26, 2012, - p.107-108.

5. Maharramov, A.M., Ramazanov, M.A., Hajiyeva, F.V. New polymer nanocomposite materials based on polyethylene and lead sulfide // Materials of the IV International Scientific Conference "Nanoscale systems: structure, properties, technologies: Nansis-2013", Kiev, Ukraine: - November 19-22, -2013, - p.547.

6. Maharramov, A.M., Ramazanov, M.A., Hajiyeva, F.V., Gulieva V.M. Investigation of the structure and electrophysical properties of nanocomposite materials based on zirconium dioxide nanoparticles in an isotactic polypropylene matrix // Materials of the IV International Scientific Conference "Nanoscale Systems: Structure, Properties, Technologies: Nansis-2013", Kiev,Ukraine: - November 19-22, -2013, - p. 546.

7. Ramazanov, M.A., Hajiyeva, F.V., Rahmatova J.R.

Investigation of nanocomposites based on polypropylene and iron nanoparticles by magnetic force microscopy // Materials of the International Scientific Conference "Actual Problems of Physics" dedicated to the 80th anniversary of Academician B.M.Askerov, Baku, Azerbaijan: - December 6, -2013, - pp. 234-235.

8. Magerramov, A.M. Study of the structure and dielectric properties of nanocomposites based on polypropylene and zirconia nanoparticles / A.M.Magerramov, M.A.Ramazanov, F.V.Hajiyeva // Surface Engineering and Applied Electrochemistry,- 2013. 49(5), -p.355-358.

9. Magerramov, A.M. Investigation of structure and electrophysical properties of nanocomposite materials on the basis of zirconium dioxide in isotactic polypropylene matrix / A.M.Magerramov, M.A.Ramazanov, F.V.Hajiyeva, V.M.Guliyeva // Journal of Ovonic Research, - 2013. 9(5), - p.133-141.

10. Ramazanov, M.A., Hajiyeva, F.V. Luminescent properties of nanocomposites based on isotactic polypropylene (PP) and zirconium dioxide nanoparticles (ZrO_2) // Materials of the IV International Scientific Conference "Nanostructures in Condensed Matter", Minsk, Belarus: - October 7-10, - 2014, - pp. 352-353.

11. Magerramov, A.M. Structure and dielectric properties of nanocomposites on the basis of high-density polyethylene and lead sulfide / A.M.Magerramov, M.A.Ramazanov, F.V.Hajiyeva // Chalcogenide Letters, - 2014. 11(4), -p.175-180.

12. Hajiyeva, F.V., Rahimli, A.M. Investigation of the structure of nanocomposites based on polyvinylidene fluoride (PVDF) and zirconium dioxide nanoparticles (ZrO_2) // Materials of the Republican Scientific Conference "Actual Problems of Physics, Baku, Azerbaijan: -17 December, - 2015, - p. 219-222.

13. Ahmedova, A.B., Hajiyeva, F.V., Ramazanov, M.A. Dielectric properties of nanocomposites based on isotactic polypropylene and titanium nanoparticles // Materials of the Republican Scientific Conference "Actual Problems of Physics, Baku, Azerbaijan: -17 December, - 2015, -p.200-202.

14. Hajiyeva, F.V. Luminescent properties of nanocomposites on the basis of isotactic polypropylene and zirconium dioxide

nanoparticles / F.V.Hajiyeva, M.A.Ramazanov, A.M.Maharramov // Nanomedicine & Nanotechnology,- 2015. 7, - p.1-3.

15. Ramazanov, M.A. Influence of electrothermopolarization on structure and photoluminescent properties of polypropylene and MnO_2-based nanocompositions / M.A.Ramazanov, A.S.Huseynova, F.V.Hajiyeva // Journal of Ovonic Research,- 2015. 11(1), - p.35-39.

16. Ramazanov, M.A. Morphology, mechanical and thermal properties of nanocomposites based on isotactic polypropylene and zirconium dioxide nanoparticles / M.A.Ramazanov, A.M.Maharramov, F.V.Hajiyeva, F.Kıraç, O.Güven // Revista Română de Materiale/Romanian Journal of Materials,- 2016. 46 (3), - p.375-382.

17. Maharramov, A.M. Investigation the structure and dielectric properties of PP+PbS nanocomposites synthesized on the basis of polypropylene polymer irradiated by accelerated heavy ions / A.M.Maharramov, M.A.Ramazanov, F.V.Hajiyeva, S.S.Amirov // Journal of Optoelectronics and Biomedical Materials,- 2016. 8(1),- p.15-20.

18. Maharramov, A.M. A structure and dielectric properties of nanocomposites based on isotactic polypropylene and lead sulphide nanoparticles / A.M.Maharramov, M.A.Ramazanov, F.V.Hajiyeva // Journal Chalcogenide Letters, - 2016. 13(1),- p. 35-40.

19. Ramazanov, M.A. Influence of corona discharge on the electret and charge states of nanocomposites based on isotactic polypropylene and zirconium dioxide nanoparticles / M.A.Ramazanov, F.V.Hajiyeva, A.M.Maharramov // J. Ferroelectrics,- 2016. 493 (1), - p. 103-109.

20. Shirinova, H. Synthesis and characterization of magnetic nanocomposites for environmental remediation / H.Shirinova, L.Palma, F.Sarasini, J.Tirillò, M.A. Ramazanov, F.V.Hajiyeva, D.Sannino, M.Polichetti, A.Galluzzi // Chemical Engineering Transactions,- 2016. 47,-p.103-108.

21. Kisyelova, T. Effect of the reactor configuration on the production of silver nanoparticles / T.Kisyelova, A.Novruzova, F.V.Hajiyeva, M.A.Ramazanov, A.Chianese // Chemical Engineering Transactions, -2016. 47,- p. 121-126.

22. Ahmedova, A.B. Structural, thermogravimetric and mechanical analysis of nanocomposites based on polyvinylidene fluoride and titanium nanoparticles / A.B.Ahmedova, M.A.Ramazanov, F.V.Hajiyeva // News of Baku University, - 2016.4, - p. 133-142.

23. Ramazanov, M.A. Dielectric properties of polymer nanocomposite materials based on polyvinylidene fluoride and titanium nanoparticles / M.A.Ramazanov, F.V.Hajiyeva, A.B. Ahmedova // News of Baku University, - 2016.2, - p. 133-142.

24. Ahmedova, A.B., Ramazanov, M.A., Hajiyeva, F.V. Luminescent properties of nanocomposites based on PP+TiO$_2$ // Materials of the IX Republican Scientific Conference "Actual Problems of Physics, Baku, Azerbaijan: -22 December, -2016, - p.183-186.

25. Ramazanov, M.A., Hajiyeva, F.V., Shirinova, H.A., Hasanova, M.R. DSC study of nanocomposites based on isotactic polypropylene and magnetite nanoparticles // Materials of the IX Republican Scientific Conference "Actual Problems of Physics, Baku, Azerbaijan: -22 December, -2016, - p. 179-181.

26. Ramazanov, M.A., Hajiyeva, F.V., Novruzova, A.A., Maharramova, G.Y. Synthesis and optical properties of PP+PbS/CdS hybrid nanocomposites // Materials of the IX Republican Scientific Conference "Actual Problems of Physics, Baku, Azerbaijan: -22 December, -2016, -p. 177-178.

27. Ramazanov, M.A., Ahmedova, A.B., Hajiyeva, F.V., Rahimli, A.M., Nuriev, M.A. Influence of polarization processes under the action of a corona discharge on the electret properties and charge state of polymer nanocomposites based on PP+TiO$_2$ // Materials of the I International Conference of Young Researchers, dedicated to the 94th anniversary of the national leader Heydar Aliyev, Baku, Azerbaijan: - 05-06 May, -2017, -p.51-52.

28. Ramazanov, M.A. Influence of polarization charges on the photoluminescence properties of nanocomposites based on polyvinylidene fluoride and titanium dioxide nanoparticles / M.A.Ramazanov, F.V.Hajiyeva, A.M.Maharramov, A.M.Rahimli // Journal of Inorganic and Organometallic Polymers and Materials,-

2017. 27(1), - p.239-243.

29. Maharramov, A.M. Structure and thermic properties of polymer nanocomposites on the basis polypropylene and silver sulphide nanoparticles PP/Ag$_2$S / A.M.Maharramov, M.A.Ramazanov, S.G.Nuriyeva, F.V.Hajiyeva // Journal of Low Dimensional Systems,- 2017. 1(1), - p.14-19.

30. Magerramov, A.M., Ramazanov, M.A., Hajiyeva, F.V., Nuriyeva, S.G. Structure and dielectric properties of polymer nanocomposites on the basis of polypropylene and silver sulfide PP/Ag$_2$S // International Conference "Modern trends in physics", Baku, Azerbaijan: 20-22 April,- 2017.- p.7-11.

31. Palma, L. Effect of nano-magnetite particle content on mechanical, thermal and magnetic properties of polypropylene composites / L.Palma, I.Bavasso, F.Sarasini, J.Tirillò, D.Puglia, F.Dominici, L.Torre, A.Galluzzi, M.Polichetti, M.A.Ramazanov, F.V.Hajiyeva, H.A.Shirinova // Polymer Composites,- 2018. 39(S3), - p.1742-1750.

32. Valadova, G.P., Babaev, Y.A., Ramazanov, M.A., Hajiyeva, F.V. Preparation and properties of polymer nanocomposites based on polyvinyl chloride and zinc sulfide nanoparticles // Materials of the International Scientific Conference of Young Scientists "Problems of Physics and Astronomy", Baku, Azerbaijan: May 24-25, -2018.- p. 255-257.

33. Ramazanov, M.A. Theoretical and experimental investigation of the magnetic properties of polyvinylidene fluoride and magnetite nanoparticles-based nanocomposites / M.A.Ramazanov, A.M.Maharramov, R.A.Alizada, H.A.Shirinova, F.V.Hajiyeva // Journal of Theoretical and Applied Physics, -2018. 12 (1), - p.7-13.

34. Ramazanov, M.A. The effect of the temperature–time mode of crystallization on the morphology and thermal properties of nanocomposites based on polypropylene and magnetite / M.A.Ramazanov, A.M.Maharramov, F.V.Hajiyeva, H.A.Shirinova, L.Palma // Journal of Inorganic and Organometallic Polymers and Materials, -2018. 28(3), - p.1171-1177.

35. Maharramov, A.M. Influence of magnetite nanoparticles on the dielectric properties of metal oxide/polymer nanocomposites

based on polypropylene / A.M.Maharramov, M.A.Ramazanov F.V.Hajiyeva, H.A.Shirinova, L.Palma //Russian Physics Journal,- 2018. 60(9), p.1572-1576.

36. Ramazanov, M.A. Electrophysical parameters of PP+Fe$_3$O$_4$ based nanocomposites depending on temperature-time mode of crystallization / M.A.Ramazanov F.V.Hajiyeva, H.A.Shirinova, A.M.Maharramov, L.Palma // Proceedings of Problems Physics and Astronomy, Baku, Azerbaijan: 28 may,- 2018,-p.57-60.

37. Ramazanov, M.A. Thermal and mechanical properties of PP+Fe and PVDF+Fe based nanocomposites / M.A.Ramazanov, A.M.Maharramov, F.V.Hajiyeva, J.R.Sultanova // Journal of Optoelectronics and biomedical materials,-2018. 10(3), - p. 83-90.

38. Ramazanov, M.A. Theoretical and experimental study of the magnetic properties and size of distribution of PVDF+Fe based nanocomposites / Ramazanov M.A., Alizade R.A., Maharramov A.M., Hajiyeva F.V., Sultanova J.R., Shirinova H.A. // Journal of Inorganic and Organometallic Polymers and Materials, - 2018. 28(5), - p. 2179-2186.

39. Ramazanov, M.A., Hajiyeva, F.V., Maharramov, A.M., Shirinova, H.A., Babayev, Y.A., Valadova, G. Structure and optical properties of polymer nanocomposites based on PVC+ZnS // Proceedings of Problems Physics and Astronomy, Baku, Azerbaijan: 28 may,- 2018,- p.30-36

40. Ramazanov, M.A. Influence of crystallization temperature–time technological factors on structure and photoluminescent properties of polymer nanocomposites on the base of isotactic polypropylene (PP) and lead sulphide (PbS) nanoparticles / M.A.Ramazanov, F.V.Hajiyeva // Journal of Inorganic and Organometallic Polymers and Materials,-2019. 29 (6),- p.2168–2175.

41. Ramazanov, M.A., Chianese, A., Hajiyeva, F.V., Novruzova, A.A. Influence of thermal treatment on photoluminescencent properties of PP/PbS/CdS nanocomposites // Materials of International Conference "Modern trends in physics", Baku, Azerbaijan: 01-03 May,- 2019,- p.67.

42. Ramazanov, M.A., Ibrahimova, H.S., Hajiyeva, F.V.

Influence of electrothermopolarization conditions on strength and electret properties of PP+ZrO$_2$ nanocompositions // Materials of International conference «Modern trends in physics», Baku, Azerbaijan: 01-03 May,- 2019,- p.76.

43. Ramazanov, M.A., Hajiyeva, F.V. Synthesis and structure of hybrid polymer nanocomposites based on PP+CdS/ZnS // Materials of International conference «Modern trends in physics», Baku, Azerbaijan: 01-03 May,- 2019,- p.75.

44. Ramazanov, M.A. Metallopolymer nanocomposites based on PP/Ni: structure and electrophysical properties / M.A.Ramazanov, F.V.Hajiyeva // Acta Physica Polonica A, -2019. 136(3), - p.513-519.

45. Ramazanov, M.A. Structure and magnetic properties of PP+Fe$_3$O$_4$ nanocomposites depending on manucturing techniques / M.A.Ramazanov, F.V.Hajiyeva, H.A.Shirinova, A.Kh.Karimova // International Journal of Modern Physics B, -2019. 33(27),-p.1950315

46. Ramazanov, M.A. Influence of temperature-time mode of crystallization on electrophysical characteristics of the polypropylene/magnetite nanocomposite / M.A.Ramazanov, H.A.Shirinova, F.V.Hajiyeva, A.Kh.Karimova // Integrated Ferroelectrics, - 2019. 201(1),-p.218-223.

47. Ramazanov, M.A. Structure and photoluminescence properties of hybrid nanocomposites on the base of PP/PbS/CdS / M.A.Ramazanov, A.Chianese, F.V.Hajiyeva, A.A.Novruzova // J. Integrated Ferroelectrics, -2019. 201(1), -p.55-61

48. Hajiyeva, F.V. Magnetic nanocomposites: preparation and characterization of polymer-coated iron oxide nanoparticles // Journal of Low Dimensional Systems, - 2019. 3(2), - p.49-53.

49. Hajiyeva, F.V. Hybrid semiconductor polymer nanocomposites and methods of their formation //Power Engineering Problems, -2019. №.4, - p.36-43.

50. Hajiyeva, F.V. Synthesis and stabilization of metal nanoparticles of iron, nickel and cobalt // Journal of Baku Engineering University, -2019. 3(1), -p.3-7.

51. Hajiyeva, F.V. Synthesis and structure of hybrid polymer nanocomposites based on PP+CdS/ZnS // Conference proceedings «Modern trends in physics», Baku, Azerbaijan: - 1-3 May, - 2019, -

p.102-108.

52. Ramazanov, M.A. Influence of electrothermopolarization conditions on strength and electret properties of $PP+ZrO_2$ nanocompositions / M.A.Ramazanov, H.S.Ibrahimova, F.V.Hajiyeva // Conference proceedings «Modern trends in physics», Baku, Azerbaijan: 01-03 May,- 2019,- p.76-79.

53. Ramazanov, M.A. The relation between the composition, structure and absorption properties of ultra-high frequency radio waves of poly (vinylidene fluoride) /magnetite nanocomposites / M.A.Ramazanov, F.V.Hajiyeva, H.A.Shirinova, H.M.Mamedov // International Journal of Modern Physics B, -2019. 33(10), - p.1950083.

54. Ramazanov, M.A. Negative magnetoresistance of polymer nanocomposites on the basis of $PP+Fe_3O_4$ and $PVDF+Fe_3O_4$ in the magnetic field / M.A.Ramazanov, A.M.Maharramov, L.Palma, H.A.Shirinova, F.V.Hajiyeva, M.R.Hasanova // Journal Ferroelectrics,-2019. 537(1),-p.191-197.

55. Ramazanov, M.A. Structure and properties of PP/TiO_2 based polymer nanocomposites / M.A.Ramazanov, F.V.Hajiyeva, A.M.Maharramov // Journal Integrated Ferroelectrics, -2019. 192(1),- p.103-112.

56. Ramazanov, M.A. Microwave absorption of polymer nanocomposites on the base high-density polyethylene and magnetite nanoparticles / M.A.Ramazanov, A.M.Maharramov, F.V.Hajiyeva, H.M.Mamedov // Journal of Elastomers&Plastics,- 2019. 51(2),- p.130-142.

57. Ramazanov, M.A. Synthesis and optical properties of PVC-CdS-based nanocomposites / M.A.Ramazanov, F.V.Hajiyeva, Y.A.Babayev, G.V.Valadova, S.G.Nuriyeva, H.A.Shirinova // Journal of Elastomers&Plastics, - 2020. 52(2), -p.159-166.

58. Ramazanov, M.A. Theoretical and experimental investigation of the particle size distribution and magnetic properties of the $PP+Fe_3O_4$ nanocomposites / M.A.Ramazanov, A.M.Maharramov, R.A.Alizada, H.A.Shirinova, F.V.Hajiyeva // Journal of Thermoplastic Composite Materials,- 2020. 33(1), -p.125-137

59. Ramazanov, M.A. New polymeric three phase

nanocomposites based on polyvinylidene fluoride, magnetite nanoparticles and multi-walled carbon nanotubes: production, structure and properties / M.A.Ramazanov, H.A.Shirinova, F.V.Hajiyeva, D.Bychanok // Journal of Inorganic and Organometallic Polymers and Materials, - 2020. 30,-p. 4783-4791.

60. Ramazanov, M.A. Influence of electrothermopolarization on PE+PbCrO$_4$ –based nanocomposition structures / M.A.Ramazanov, A.S.Huseynova, F.V.Hajiyeva, S.U.Atayeva // Integrated Ferroelectrics,-2020. 211(1), - p.160-166.

61. Ramazanov, M.A. Magnetic properties of the iron nanoparticles distributed in polymer matrix: theoretical and experimental approach / M.A.Ramazanov, H.A.Shirinova, F.V.Hajiyeva, J.R.Sultanova, R.A.Alizade // Acta Polonica,-2020. 138(6), - p.787-783.

62. Ramazanov, M.A. Copper and copper oxide nanoparticles in polypropylene matrix: synthesis, characterization and dielectric properties / M.A.Ramazanov, F.V.Hajiyeva // Composite Interfaces,-2020. 27(11), - p.1047-1060.

63. Ramazanov, M.A. Influence of thermal treatment on photoluminescent properties of PP/PbS/CdS nanocomposites / M.A.Ramazanov, A.Chianese, F.V.Hajiyeva, A.A.Novruzova // International Journal of Modern Physics B, - 2020. 34(6), - p.2050038.

64. Ramazanov, M.A. The impact of manufacturing technology, of the polypropylene matrix and iron oxide nanoparticles based magnetodielectric nanocomposites on electrophysical parameters / M.A.Ramazanov, H.A.Shirinova, F.V.Hajiyeva // Materials Chemistry and Physics, - 2020. 253(1), - p.123287.

65. Ramazanov, M.A. Fabrication, characterization and optical properties of transparent PP/yttria-stabilizied zirconia (YSZ) based nanocomposites / M.A.Ramazanov, F.V.Hajiyeva, H.A.Shirinova // Journal of Elastomers&Plastics, -2020. 53(5), p.417-429.

66. Ramazanov, M.A. The influence of titanium dioxide (TiO$_2$) nanoparticles on the structure, optical and dielectric properties of polyvinyl chloride (PVC) / M.A.Ramazanov, A.M.Rahimli, F.V.Hajiyeva // Modern Physics Letters B,- 2020. 34(28),-p.2050310

67. Hajiyeva, F.V. New hybrid polymer nanocomposites based on polyvinylidene fluoride and CdS/ZnS nanoparticles: structure and dielecric properties // Surface Engineering and Applied Electrochemistry, - 2020. 56(6), - p.649-655.

68. Hajiyeva, F.V. Structure, optical and photoluminescent properties of hybrid polymer nanocomposites on the base PP+CdS/ZnS / F.V.Hajiyeva, M.A.Ramazanov, H.A.Shirinova // International Journal of Nano Dimension,-2021. 12 (3),-p.293-304.

69. Hajiyeva, F.V. Photosensitive hybrid polymer nanocomposites on the base PVDF+CdS/ZnS for solar cells application / F.V.Hajiyeva, M.A.Ramazanov, H.A.Shirinova, G.Y.Maharramova // Composite Interfaces,-2021,- p.1-19.

70. Hajiyeva, F.V. Influence of polarization conditions on the photoluminescent and electret properties of polymer nanocomposites based on PP+TiO$_2$ // Process of Petrochemistry and Oil (PPOR),- 2021. 22(3),-p.416-424.

71. Hajiyeva F.V. Structure and thermal properties of polymer nanocomposites based on PVDF/Cu // Journal of Baku Engineering University, - Chemistry and biology, -2021. 5(1), -p.69-78.

72. Hajiyeva F.V. Structure, electrophysical, thermal and mechanical properties of polymer nanocomposites based on polyvinylidene fluoride (PVDF) and multi-walled carbon nanotubes (MWCNT) // Advanced Physical Research,-2021. 3 (2), - p.114-122.

73. Huseynova, A.S., Hajiyeva, F.V. Relaxation properties of PP and PE-based nanocomposites // Materials of 7th International Conference MTP-2021: Modern Trends in Physics, Baku, Azerbaijan: 15-17 December, -2021,-p.112-113.

The defense will be held on February 17, 2022 at 10^{00} at the meeting of the Dissertation council under registration number BED 1.16/2 of the Supreme Attestation Commission under the President of the Republic of Azerbaijan, created on the basis of ED 1.16 of the Institute of Petrochemical Processes named after academician Y.G.Mamedaliyev of the National Academy of Sciences of Azerbaijan

Address: Azerbaijan Republic, AZ 1025, Baku city, Khojaly avenue.

Dissertation is accessible at the library of Y.H.Mamedaliyev's Institute of Petrochemical Processes of the National Academy of Sciences of Azerbaijan.

Electronic versions of dissertation and its abstract are available on the official website www.nkpi.az of the Y.H.Mamedaliyev's Institute of Petrochemical Processes.

Abstract was sent to the required addresses on January 14, 2022